RAD51-dependent recruitment of TERRA lncRNA to telomeres through R-loops

https://doi.org/10.1038/s41586-020-2815-6

Received: 13 October 2019

Accepted: 16 July 2020

Published online: 14 October 2020

Check for updates

Marianna Feretzaki[1], Michaela Pospisilova[2], Rita Valador Fernandes[1], Thomas Lunardi[1], Lumir Krejci[2,3]✉ & Joachim Lingner[1]✉

Telomeres—repeated, noncoding nucleotide motifs and associated proteins that are found at the ends of eukaryotic chromosomes—mediate genome stability and determine cellular lifespan[1]. Telomeric-repeat-containing RNA (TERRA) is a class of long noncoding RNAs (lncRNAs) that are transcribed from chromosome ends[2,3]; these RNAs in turn regulate telomeric chromatin structure and telomere maintenance through the telomere-extending enzyme telomerase[4–6] and homology-directed DNA repair[7,8]. The mechanisms by which TERRA is recruited to chromosome ends remain poorly defined. Here we develop a reporter system with which to dissect the underlying mechanisms, and show that the UUAGGG repeats of TERRA are both necessary and sufficient to target TERRA to chromosome ends. TERRA preferentially associates with short telomeres through the formation of telomeric DNA–RNA hybrid (R-loop) structures that can form in *trans*. Telomere association and R-loop formation trigger telomere fragility and are promoted by the recombinase RAD51 and its interacting partner BRCA2, but counteracted by the RNA-surveillance factors RNaseH1 and TRF1. RAD51 physically interacts with TERRA and catalyses R-loop formation with TERRA in vitro, suggesting a direct involvement of this DNA recombinase in the recruitment of TERRA by strand invasion. Together, our findings reveal a RAD51-dependent pathway that governs TERRA-mediated R-loop formation after transcription, providing a mechanism for the recruitment of lncRNAs to new loci in *trans*.

TERRA is transcribed from numerous chromosome ends, and comprises both subtelomeric sequences and telomeric repeats. More than 50% of TERRA is associated with chromatin[9]. To investigate how TERRA is recruited to or retained at telomeres, we generated a plasmid encoding 24 copies of the stem-loop of phage PP7 (ref. [10]) under the control of the tetracycline-inducible (TET) promoter, followed by 90 TTAGGG repeats (Fig. 1a). To generate full-length TERRA transcripts, we also cloned the human chromosome Xq and 15q subtelomeric regions containing the TERRA start sites between the PP7 stem-loops and the TTAGGG repeats. The constructs were then transiently transfected into HeLa clones that were constitutively expressing the PP7 coat protein fused to GFP (PCP–GFP) and a nuclear-localization signal. PCP–GFP exhibited a diffuse signal in the nucleus but formed nuclear foci upon expression of the PP7 stem-loops, which are bound by PCP and can gather up to 48 PCP–GFP molecules per RNA. These foci did not co-localize with telomeres (Fig. 1b). The fusion of the subtelomeric region of 15q or Xq TERRA to the stem-loops did not promote substantial trafficking of the PP7 foci to telomeres. However, when the telomeric TTAGGG repeats were fused downstream of PP7, co-localization with telomeres occurred, as analysed by conventional and confocal imaging (Fig. 1b), indicating that the 5′-UUAGGG-3′ repeats of TERRA drive telomere association. The full-length PP7-tagged 15q and Xq chimaeric TERRA also showed marked co-localization with telomeres (Fig. 1b and Extended Data Fig. 1a). Therefore, chimaeric TERRAs that originated from a plasmid were directed to telomeres in *trans*.

To eliminate possible confounding effects due to the high plasmid copy number or increased levels of transgenic TERRA, we used CRISPR–Cas9 technology to integrate the chimaeric TERRA constructs into the genome at the adeno-associated-virus integration site 1 (AAVS1) on chromosome 19, which represents a safe harbour for transgene expression[11] (Extended Data Fig. 1b). Following isolation of clones, we confirmed monoallelic site-specific integration of the full constructs by polymerase chain reaction (PCR) and sequencing. These TERRA expression levels were lower than the levels of expression from plasmids, giving one to three foci—indicative of displacement from the transcription site. But, similar to the results obtained upon transient transfection, the PP7 loops formed nuclear foci, and only when fused to 5′-UUAGGG-3′ repeats did the chimaeric RNAs co-localize with telomeres (Extended Data Fig. 1c, d).

Shorter telomeres recruit more TERRA

In *Saccharomyces cerevisiae* and *Schizosaccharomyces pombe*, short telomeres recruit more TERRA, possibly to facilitate telomere maintenance through recombination or telomerase recruitment[5,6,8]. To explore the putative roles of telomere length in TERRA recruitment

[1]Swiss Institute for Experimental Cancer Research (ISREC), School of Life Sciences, Ecole Polytechnique Fédérale de Lausanne (EPFL), Lausanne, Switzerland. [2]Department of Biology and National Centre for Biomolecular Research, Masaryk University, Brno, Czech Republic. [3]International Clinical Research Center, St Anne's University Hospital, Brno, Czech Republic. ✉e-mail: lkrejci@chemi.muni.cz; joachim.lingner@epfl.ch

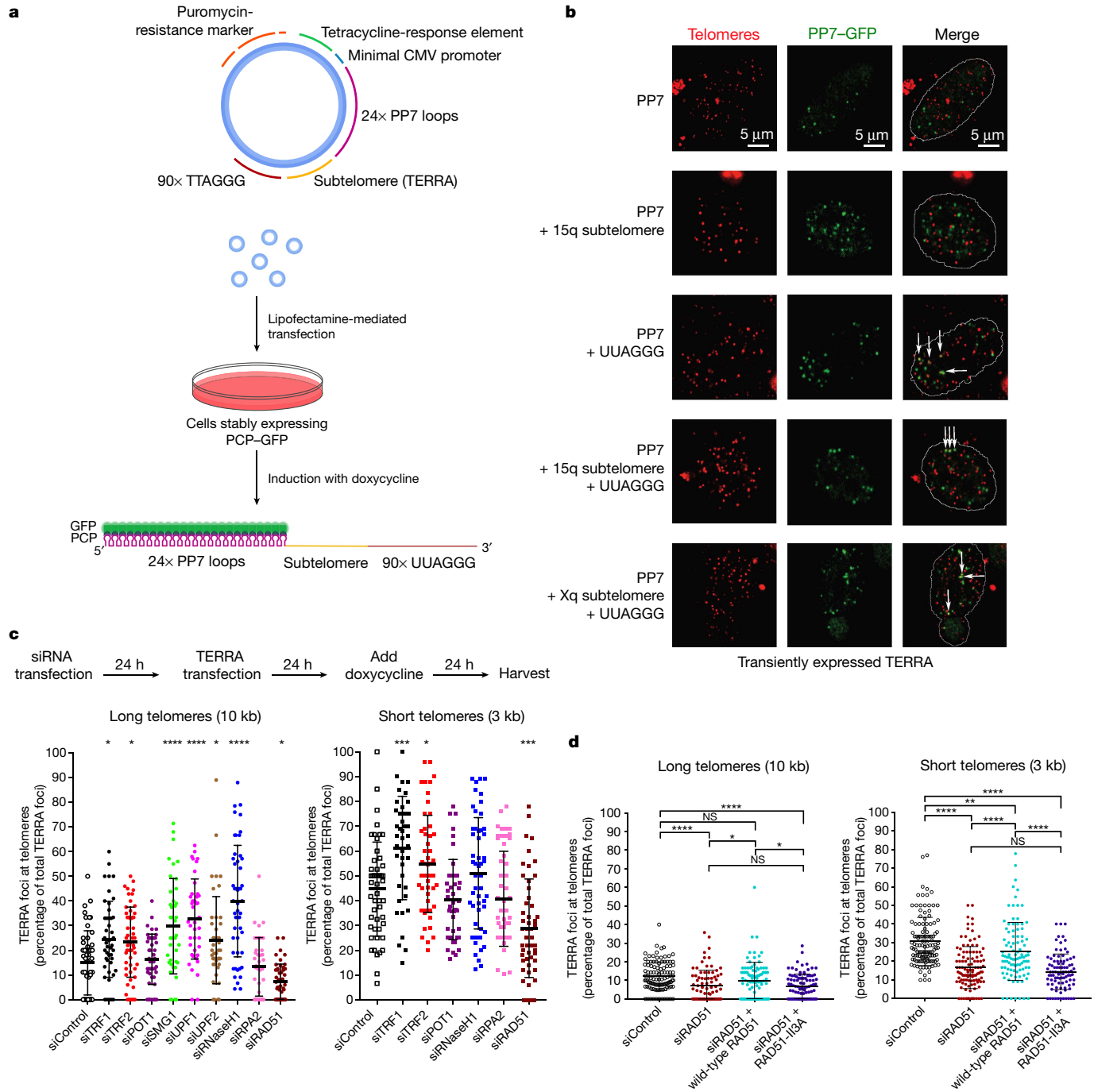

Fig. 1 | Transgenic TERRA associates with telomeres in a manner that depends on RAD51. a, Chimaeric TERRA construct (top) and assay for TERRA localization (bottom). Using lipofectamine, plasmids were transfected into HeLa cells constitutively expressing PCP–GFP protein. After 24 h, transcription of TERRA was induced with doxycycline. Chimaeric TERRA, which is recognized and bound by PCP–GFP, was analysed 24 h after induction. CMV, cytomegalovirus. **b**, Fluorescence in situ hybridization (FISH) analysis of telomeric DNA (red) and immunofluorescence of GFP (green) were used to assess the co-localization of transiently expressed PP7 constructs with telomeres. Confocal images are shown. White arrows indicate co-localization of PP7 foci with telomeric signals. **c**, To identify proteins involved in the localization of TERRA at telomeres, we used siRNAs to target factors implicated in TERRA and telomere biology. HeLa clones with long (10-kilobase average) and short (3 kb) telomeres were transfected first with siRNA pools and then with chimaeric TERRA. The percentage of co-localizing TERRA foci was assessed by telomeric FISH combined with GFP immunofluorescence. $n = 2$ biologically independent experiments; more than 40 nuclei were analysed per condition; data are means ± s.d. One-way analysis of variance (ANOVA) with Dunnett's multiple comparisons test was used, comparing all conditions with control siRNA (siControl): $^{*}P < 0.05$; $^{**}P < 0.01$; $^{***}P < 0.001$; $^{****}P < 0.0001$. **d**, The enzymatic activity of RAD51 is required to recruit TERRA. Endogenous RAD51 was depleted with siRNA, and wild-type RAD51 or the RAD51 II3A mutant was expressed from plasmid containing complementary DNA. The co-localization of TERRA with telomeres was assessed as in **c**. $n = 3$ biologically independent experiments; more than 80 nuclei were analysed per condition; data are means ± s.d. A two-tailed unpaired t-test was used to calculate P-values: $^{*}P < 0.05$; $^{**}P < 0.01$; $^{***}P < 0.001$; $^{****}P < 0.0001$.

in human cells, we isolated individual HeLa clones that constitutively expressed the PCP–GFP and measured telomere lengths by telomere restriction fragment length (TRF) analysis (Extended Data Fig. 2). Cells carrying short telomeres recruited TERRA much more efficiently than cells with long telomeres, as seen upon transient or stable expression of TERRA (Extended Data Fig. 2). Therefore, short telomeres must be

more accessible to recruitment or retention of TERRA; alternatively, long telomeres might contain active systems that expel TERRA. In both experiments the overall expression levels of chimaeric TERRA varied in individual clones, but this did not correlate with telomere length and telomere recruitment of TERRA (Extended Data Fig. 2b, d).

Recombination factors enable TERRA recruitment

To identify proteins involved in the localization of TERRA at telomeres, we performed screens using short interfering RNAs (siRNAs) to target selected factors implicated in TERRA and telomere biology. Using cell lines with long or short telomeres, we transfected first siRNA pools and then the 15q TERRA construct. After inducing TERRA expression with doxycycline, we analysed the cells (Fig. 1c) and evaluated the level of depletion of each factor by using reverse transcription with quantitative PCR (RT–qPCR) or western blotting (Extended Data Fig. 3a, b). We found that the number of transgenic TERRA foci was not affected by individual depletions, and we observed no striking effects on levels of selected endogenous TERRA molecules (Extended Data Fig. 3c, d). Among tested factors, depletion of telomeric repeat factor 1 (TRF1) significantly increased TERRA co-localization at short and long telomeres, while removal of TRF2 led to a milder increase in recruitment (Fig. 1c). Depletion of the nonsense-mediated decay (NMD) factors also stimulated co-localization of TERRA at long telomeres, supporting their crucial role in displacing TERRA from chromosome ends[2]. Similarly, removal of RNaseH1 resulted in a substantial accumulation of TERRA at chromosome ends in cells with long telomeres (Fig. 1c). This result indicated that TERRA recruitment to, or retention at, long telomeres involves the formation of DNA–RNA hybrids. In cells with short telomeres, depletion of RNaseH1 only marginally increased the co-localization of TERRA with telomeres. The roles of NMD factors in cells with short telomeres could not be analysed, as their depletion caused cell death. Notably, depletion of RAD51—which facilitates strand invasion of DNA molecules during homology-directed repair (HDR)—led to a substantial decrease in TERRA recruitment to both long and short telomeres (Fig. 1c, d).

The involvement of RAD51 in TERRA recruitment prompted us to interrogate the role of the BRCA2 protein in TERRA trafficking. BRCA2 loads RAD51 and promotes the displacement of replication protein A (RPA), allowing the formation of stable filaments of RAD51 on single-stranded DNA (ssDNA) that are capable of homology search to facilitate HDR during double-strand-break repair; BRCA2 also protects stalled replication forks[12,13]. We found that depletion of BRCA2 led to a marginal decrease in TERRA recruitment at long, but more prominent reduction at short, telomeres (Extended Data Fig. 4a). However, removal of BRCA2 also diminished total RAD51 protein levels in both cell lines (Extended Data Fig. 4a). Finally, we tested whether RAD51 enzymatic activity is required for TERRA recruitment, taking advantage of a mutation (RAD51 II3A) that allows the protein to retain its DNA-binding but not its strand-invasion activity[14]. In siRAD51-treated cells, the expression of wild-type RAD51 from complementary DNA largely rescued TERRA co-localization with telomeres, but expression of RAD51 II3A did not (Fig. 1d and Extended Data Fig. 4b). Therefore, the enzymatic activity of RAD51 is required for TERRA to associate with telomeres. Overall, these data suggest that the HDR machinery promotes the recruitment of TERRA to telomeres.

TERRA forms R-loops causing telomere fragility

As the association of TERRA with long telomeres was increased upon depletion of RNaseH1, we hypothesized that the transgenic TERRA may form R-loops with telomeres in *trans*. To explore this possibility, we applied the DNA–RNA immunoprecipitation protocol (DRIP), in which the specificity of the S9.6 monoclonal antibody for eight to nine base pairs of DNA–RNA hybrids is exploited[15]. Precipitated nucleic acids were probed for telomeric repeats, and, as a control for specificity, isolated nucleic acids were treated in vitro with RNaseH1 before immunoprecipitation. Abolishment of the signal upon pretreatment with RNaseH1 confirmed the specificity of the assay for telomeric R-loops (Fig. 2a). As expected, we detected R-loops at telomeres in wild-type cells (Fig. 2a). Depletion of RNaseH1 led to an increase in the number of R-loops, while its overexpression to a decrease in R-loops at both long and short telomeres (Fig. 2a and Extended Data Fig. 5a). Overexpression of chimaeric TERRA further increased the frequency of R-loops in cells with both long and short telomeres (Fig. 2a); this frequency again increased upon depletion of RNaseH1 and decreased upon its overexpression (Fig. 2a and Extended Data Fig. 5a), indicating that the transgenic TERRA formed DNA–RNA hybrids.

The DRIP assay (Fig. 2a) could not distinguish to what extent the DRIP signals for transgenic TERRA were derived from R-loops forming within the transgenic plasmid during transcription, or R-loops forming after transcription in *trans* with telomeres. To measure R-loops specifically at telomeres, we used the DRIP samples derived from HeLa cells with long telomeres (Fig. 2a), and determined the presence of four specific chromosome ends by qPCR using subtelomere-specific primers residing in immediate proximity to the terminal 5′-TTAGGG-3′ repeats (Fig. 2b). Telomeric R-loops became detectable at the ends of all four chromosomes upon depletion of RNaseH1 (Fig. 2b). Specifically, 1q, 10q and 13q subtelomeric DNA increased strongly in abundance upon expression of transgenic PP7–15qTERRA, indicating that R-loops had formed at these telomeres with PP7–15qTERRA. The 15q subtelomeric signal was enhanced even more extensively, presumably because of R-loops forming with plasmid DNA containing the 15q sequence. As with wild-type TERRA, overexpression of RNaseH1 almost completely abolished the signals, whereas RNaseH1 depletion increased R-loop abundance. We sequenced the qPCR products (Extended Data Fig. 5b), verifying the identity of products for each chromosome end. Together, these data confirmed that transgenic PP7–15qTERRA associated with telomeres in *trans* through the formation of R-loop structures.

TERRA R-loops have been implicated in interfering with telomere replication[7,16–18]; this is manifested in telomere fragility[19], characterized by the accumulation of telomeric signals in metaphase chromosomes with a smeary or discontinuous appearance (Extended Data Fig. 6a). We found that transgenic TERRA increased telomere fragility (Fig. 2c and Extended Data Fig. 6b), which was suppressed by depletion of RAD51 or overexpression of RNaseH1 but increased by depletion of RNaseH1 (Fig. 2d and Extended Data Fig. 6c, d). These results confirm that, after transcription from plasmids, TERRA forms R-loops at telomeres in *trans*.

RAD51 promotes telomeric R-loop formation

We next used the DRIP assay to test the role of RAD51 in the formation of hybrids containing endogenous TERRA at telomeres in wild-type cell lines (Fig. 2e and Extended Data Fig. 7a). While depletion of RNaseH1 led to the expected mild increase in R-loops, depletion of RAD51 caused a substantial decrease in hybrid accumulation. Even stronger reduction of R-loops was observed in RAD51-depleted cells with short telomeres, which are characterized by higher levels of DNA–RNA hybrids. Therefore, RAD51 promotes the association of endogenous TERRA with telomeres through R-loop formation.

We hypothesized either that RAD51 binds TERRA to catalyse its strand invasion into the telomeric repeats (Extended Data Fig. 7b, lower panel), or that TERRA might hybridize to exposed single-stranded telomeric DNA during RAD51-mediated HDR between telomeric DNA molecules, even in the absence of a physical interaction between TERRA with RAD51 (Extended Data Fig. 7b, upper panel). To explore these hypotheses, we performed native RNA immunoprecipitations using anti-RAD51 antibodies in HeLa cells. As a control, we also included antibodies specific for hnRNPA1, as this protein binds TERRA[4]. Immunoprecipitation of

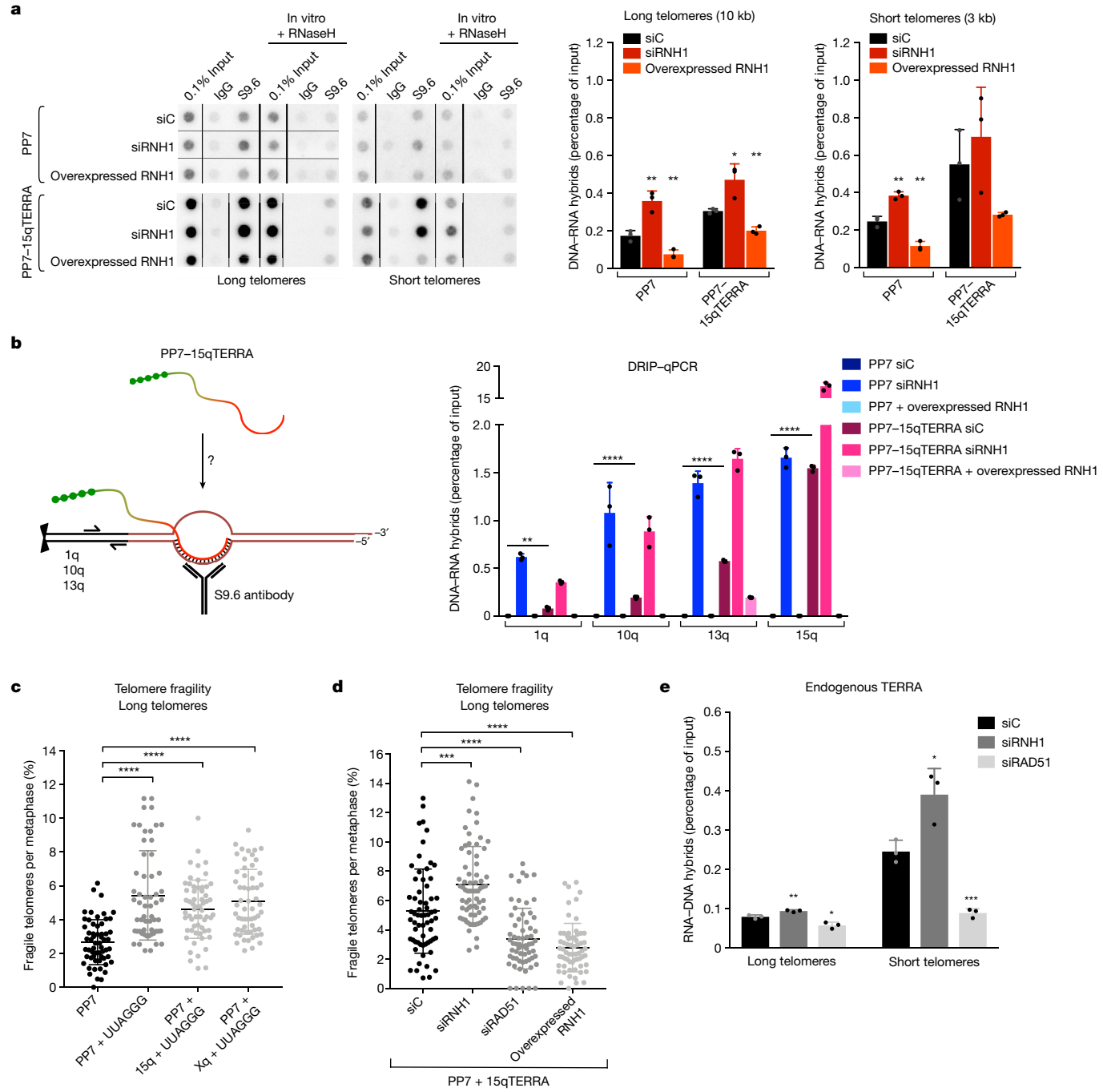

Fig. 2 | TERRA forms R-loops in *trans*, inducing telomere fragility in a RAD51-dependent way. a, Left panels, detection of telomeric hybrids on dot-blots. Telomeric hybrids were isolated from cells with long or short telomeres by DRIP using the S9.6 antibody. Cells expressed either the PP7 stem-loops or the PP7–15qTERRA, and had been transfected with control siRNA (siC), siRNAs against RNaseH1 (RNH1), or an RNH1-overexpressing plasmid. In vitro treatment with RNH1 served as a negative control. Right panels, quantification of signals. **b**, Left, schematic representation showing the expression of PP7–15qTERRA from a plasmid, forming R-loops in *trans* at telomeres 1q, 10q and 13q. Right, telomeric hybrids arising at the indicated chromosome ends were quantified by qPCR using primers that amplify specific subtelomeric DNA found next to the telomeric tracts in cells with long telomeres. **c**, Telomere fragility induced upon expression of TERRA from a plasmid. The fraction of fragile telomeres was quantified on metaphase chromosomes stained with a telomeric FISH probe (Extended Data Fig. 6). **d**, Effects of RNH1 and RAD51 on telomere fragility. In cells expressing PP7-15qTERRA from a plasmid, telomere fragility was quantified upon depletion or overexpression of RNH1, or depletion of RAD51. **e**, Detection of endogenous telomeric R-loops in cells transfected with siC, siRNH1 or siRAD51. For all panels, $n = 3$ biologically independent experiments; data are means ± s.d. Two-tailed unpaired *t*-tests were used to calculate *P*-values: *$P < 0.05$; **$P < 0.01$; ***$P < 0.001$; ****$P < 0.0001$. For **c**, **d**, the numbers of metaphases scored are indicated for each condition in Extended Data Fig. 6b, c.

endogenous RAD51 specifically retrieved TERRA and not the nuclear U1 small nuclear RNA (snRNA; Fig. 3a and Extended Data Fig. 7c), and similar results were observed in the U2OS ALT cell line (Extended Data Fig. 7d). The TERRA signal was sensitive to treatment with RNaseA, showing a specific recovery of RNA, but the RNA signal was insensitive to treatment with DNaseI. Together these results indicate that TERRA associates with RAD51 in vivo.

We wished to determine whether purified RAD51 can bind TERRA directly by carrying out electrophoretic mobility shift assays (EMSAs). We incubated recombinant RAD51 with fluorescently labelled TERRA

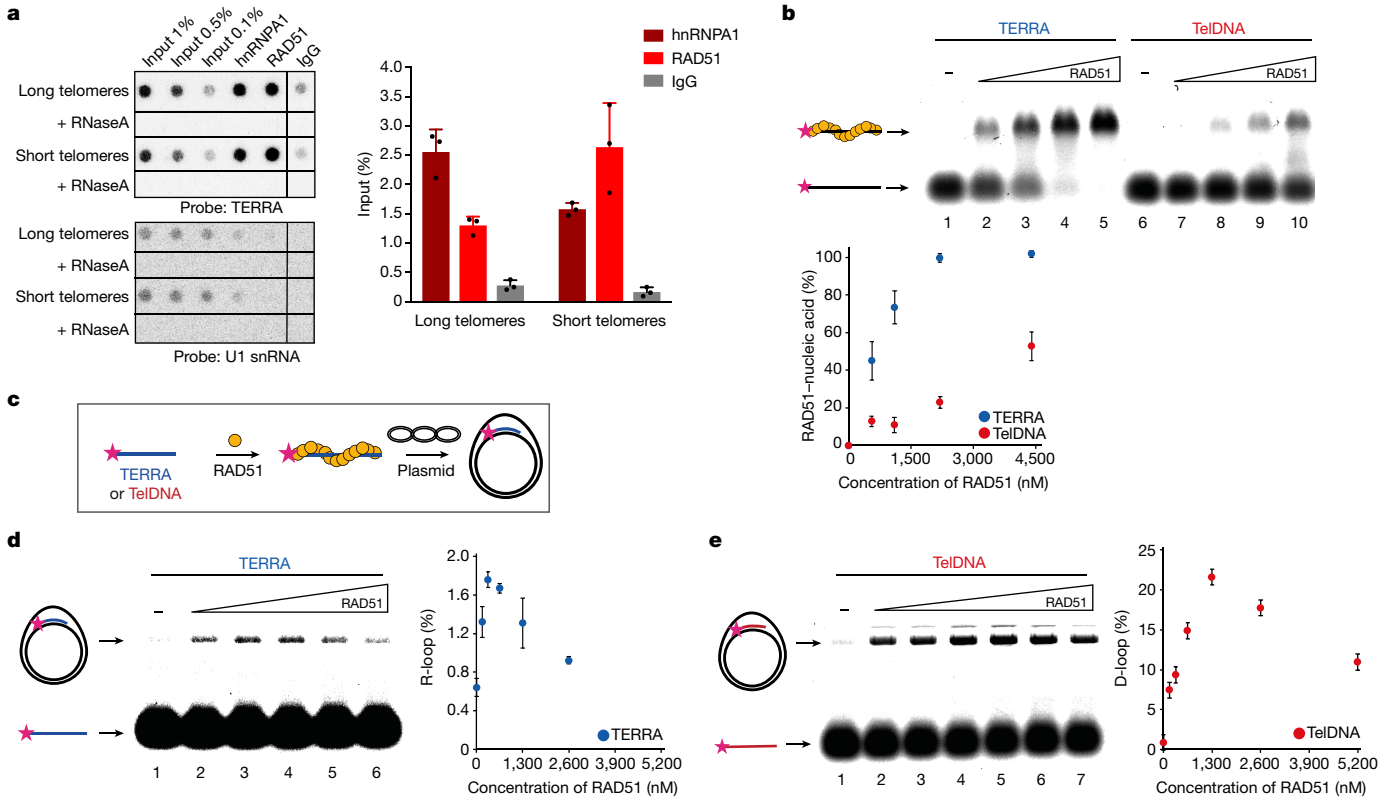

Fig. 3 | RAD51 associates with TERRA and catalyses R-loop formation. a, Native RNA-immunoprecipitation assays using anti-RAD51 and anti-hnRNPA1 antibodies were performed in extracts from HeLa cell clones with long or short telomeres. Western blotting was used to evaluate the efficiency of immunoprecipitation of RAD51 and hnRNPA1 (and the co-immunoprecipitation of BRCA2; Extended Data Fig. 7c, d). Immunoprecipitation-recovered RNA was analysed for TERRA and U1 snRNA. $n = 3$ biologically independent experiments; data are means ± s.d. **b**, The affinity of RAD51 for TERRA and telomeric DNA (TelDNA) oligonucleotides was analysed by electrophoretic mobility shift assay (EMSA). Fluorescently labelled (pink star) RNA or DNA substrates (20 nM) were incubated with increasing concentrations of RAD51 protein (0 nM, 550 nM, 1,100 nM, 2,200 nM and 4,400 nM). Quantification is shown at the bottom. $n = 3$ independent experiments; data are means ± s.d. **c**, Assay for the formation of R-loops and D-loops. **d**, The formation of R-loops depends on the concentration of RAD51: detection on native gel (left) and quantification (right). $n = 3$ independent experiments; data are means ± s.d. **e**, Detection of D-loops on native gel (left) and quantification (right). $n = 3$ independent experiments; data are means ± s.d.

or telomeric DNA oligonucleotides, and resolved the reactions by agarose-gel electrophoresis (Fig. 3b). RAD51 bound the TERRA oligonucleotide with threefold higher affinity than the corresponding telomeric DNA sequence (TelDNA), as with TERRA oligonucleotide a lower protein concentration was required to obtain shifted oligonucleotide–RAD51 complexes (Fig. 3b). The binding of RAD51 to the TERRA oligonucleotide was tighter than to an unrelated RNA (Extended Data Fig. 7e) and also more stable when compared with telomeric DNA, as shown by a stability assay in which pre-formed TERRA–RAD51 or TelDNA–RAD51 complexes were challenged with an excess of unlabelled 49-mer competitor ssDNA (cDNA) (Extended Data Fig. 7f).

To test whether RAD51 promotes R-loop formation in vitro, we carried out a strand-invasion assay using recombinant RAD51 and telomeric RNA and DNA (Fig. 3c–e). Wild-type RAD51, unlike the catalytically dead RAD51 II3A, catalysed both R-loop and D-loop formation in a concentration-dependent manner (Extended Data Fig. 8a). As expected, canonical R-loops were sensitive to treatment with RNaseH1 and were supershifted with the R-loop recognizing S9.6 antibody when combined with anti-mouse IgG (Extended Data Fig. 8b, c). Together, these data support a direct role of the RAD51 protein in localizing TERRA to initiate strand invasion and promote the formation of DNA–RNA hybrids at telomeres.

Discussion

Our data reveal the mechanism by which TERRA is recruited to chromosome ends through RNA strand invasion. The recruitment of TERRA and formation of R-loops depend on the recombinase RAD51 and the 5′-UUAGGG-3′ repeats of TERRA. Although the subtelomeric TERRA sequences were not required for telomere recruitment in our assay, we do not exclude the possibility that they may contribute by targeting endogenous TERRA molecules to their native chromosome ends. The observed base pairing between TERRA and telomeric DNA provides a mechanism for how this long noncoding RNA can encounter its major site of action at chromosome ends. Therefore, the recruitment of TERRA seems to occur through a process that strongly resembles the strand-invasion and homology-search mechanism exploited in all living organisms during DNA repair by HDR, and which is also characteristic of telomere stabilization by the ‘alternative lengthening of telomeres’ (ALT) mechanism in cancer cells. A direct involvement of RAD51 in the strand-invasion reaction is supported by our finding that RAD51 strongly binds TERRA and catalyses strand invasion into telomeric sequences in vitro. However, it is likely that there are important differences between DNA- and RNA-mediated strand invasion with the regard to the mechanism and the requirement for accessory factors, which must be explored in the future.

The increased formation of R-loops and association of RAD51 with short telomeres has previously been shown in yeast[8]. Our findings in human cells are consistent with these observations. Furthermore, we reveal that TERRA can form R-loops post-transcriptionally at telomeres in *trans*. R-loops have generally been assumed to form only during transcription, through the unsuccessful removal of native RNA from its DNA template[20]. However, previous studies in yeast suggested that

R-loops may also form at loci that are distinct from the site of synthesis of the RNA[21]. Our work here suggests that R-loop formation in *trans* plays a major part in telomere homeostasis. Through its mechanism of recruitment, TERRA may represent a scaffold that guides and regulates telomerase, HDR proteins and chromatin modifiers specifically at the chromosome ends that may need their attention. It will be interesting to see which other lncRNAs are recruited to their sites of action through similar mechanisms.

Online content

Any methods, additional references, Nature Research reporting summaries, source data, extended data, supplementary information, acknowledgements, peer review information; details of author contributions and competing interests; and statements of data and code availability are available at https://doi.org/10.1038/s41586-020-2815-6.

1. Maciejowski, J. & de Lange, T. Telomeres in cancer: tumour suppression and genome instability. *Nat. Rev. Mol. Cell Biol.* **18**, 175–186 (2017).
2. Azzalin, C. M., Reichenbach, P., Khoriauli, L., Giulotto, E. & Lingner, J. Telomeric repeat containing RNA and RNA surveillance factors at mammalian chromosome ends. *Science* **318**, 798–801 (2007).
3. Schoeftner, S. & Blasco, M. A. Developmentally regulated transcription of mammalian telomeres by DNA-dependent RNA polymerase II. *Nat. Cell Biol.* **10**, 228–236 (2008).
4. Redon, S., Zemp, I. & Lingner, J. A three-state model for the regulation of telomerase by TERRA and hnRNPA1. *Nucleic Acids Res.* **41**, 9117–9128 (2013).
5. Cusanelli, E., Romero, C. A. P. & Chartrand, P. Telomeric noncoding RNA TERRA is induced by telomere shortening to nucleate telomerase molecules at short telomeres. *Mol. Cell* **51**, 780–791 (2013).
6. Moravec, M. et al. TERRA promotes telomerase-mediated telomere elongation in *Schizosaccharomyces pombe*. *EMBO Rep.* **17**, 999–1012 (2016).
7. Arora, R. et al. RNaseH1 regulates TERRA-telomeric DNA hybrids and telomere maintenance in ALT tumour cells. *Nat. Commun.* **5**, 5220 (2014).
8. Graf, M. et al. Telomere length determines TERRA and R-loop regulation through the cell cycle. *Cell* **170**, 72–85 (2017).
9. Porro, A., Feuerhahn, S., Reichenbach, P. & Lingner, J. Molecular dissection of telomeric repeat-containing RNA biogenesis unveils the presence of distinct and multiple regulatory pathways. *Mol. Cell. Biol.* **30**, 4808–4817 (2010).
10. Larson, D. R., Zenklusen, D., Wu, B., Chao, J. A. & Singer, R. H. Real-time observation of transcription initiation and elongation on an endogenous yeast gene. *Science* **332**, 475–478 (2011).
11. Hockemeyer, D. et al. Efficient targeting of expressed and silent genes in human ESCs and iPSCs using zinc-finger nucleases. *Nat. Biotechnol.* **27**, 851–857 (2009).
12. Jensen, R. B., Carreira, A. & Kowalczykowski, S. C. Purified human BRCA2 stimulates RAD51-mediated recombination. *Nature* **467**, 678–683 (2010).
13. Thorslund, T. et al. The breast cancer tumor suppressor BRCA2 promotes the specific targeting of RAD51 to single-stranded DNA. *Nat. Struct. Mol. Biol.* **17**, 1263–1265 (2010).
14. Mason, J. M., Chan, Y.-L., Weichselbaum, R. W. & Bishop, D. K. Non-enzymatic roles of human RAD51 at stalled replication forks. *Nat. Commun.* **10**, 4410 (2019).
15. Boguslawski, S. J. et al. Characterization of monoclonal antibody to DNA.RNA and its application to immunodetection of hybrids. *J. Immunol. Methods* **89**, 123–130 (1986).
16. Sagie, S. et al. Telomeres in ICF syndrome cells are vulnerable to DNA damage due to elevated DNA:RNA hybrids. *Nat. Commun.* **8**, 14015 (2017).
17. Pfeiffer, V., Crittin, J., Grolimund, L. & Lingner, J. The THO complex component Thp2 counteracts telomeric R-loops and telomere shortening. *EMBO J.* **32**, 2861–2871 (2013).
18. Balk, B. et al. Telomeric RNA-DNA hybrids affect telomere-length dynamics and senescence. *Nat. Struct. Mol. Biol.* **20**, 1199–1205 (2013).
19. Sfeir, A. et al. Mammalian telomeres resemble fragile sites and require TRF1 for efficient replication. *Cell* **138**, 90–103 (2009).
20. Crossley, M. P., Bocek, M. & Cimprich, K. A. R-loops as cellular regulators and genomic threats. *Mol. Cell* **73**, 398–411 (2019).
21. Wahba, L., Gore, S. K. & Koshland, D. The homologous recombination machinery modulates the formation of RNA–DNA hybrids and associated chromosome instability. *eLife* **2**, e00505 (2013).

Methods

No statistical methods were used to predetermine sample size. The experiments were not randomized and investigators were not blinded to allocation during experiments and outcome assessment.

Cell culture and transfections

The telomerase-positive cell line HeLa (cervical cancer) was from the American Type Culture Collection (ATCC), and the ALT cell line U2OS (osteosarcoma) from the European Collection of Authenticated Cell Cultures (ECACC). The cells were cultured in Dulbecco's modified Eagle's medium (DMEM) supplemented with 10% fetal bovine serum (FBS) and 100 U ml^{-1} of penicillin/streptomycin (Thermo Fisher Scientific). The cell lines were maintained in a 5% CO_2 incubator at 37 °C and were routinely checked to ensure that they remained mycoplasma-free.

HeLa cells were transfected with lipofectamine 2000 according to the manufacturer's instructions (Invitrogen). To induce TERRA transcription, doxycycline (1 μg ml^{-1}) was added to the medium 24 h after transfection, and the cells were harvested 48 h after transfection. To isolate clones containing integrated TERRA transgenes, puromycin (1 μg ml^{-1}) was added to the medium 24 h following transfection using the pSpCas9(BB)-2A-Puro plasmid. Selection was maintained for 5 days. SiRNAs were purchased as pools from Dharmacon (siGENOME SMARTpool; Extended Data Table 1). Cells were transfected with 20 pmol siRNAs using calcium phosphate transfection in 6-well plates in DMEM supplemented with 10% FBS. Cells were harvested 72 h after transfection. Wild-type RAD51 or the RAD51 II3A mutant was expressed from plasmid containing complementary DNA[14].

Lentivirus production and cell transduction

Plasmids pMD2.G (1 μg) and pCMVR8.74 (3 μg) (gifts from D. Trono, EPFL) were mixed with PP7_eGFP (3 μg) (a gift from D. Larson, National Institutes of Health (NIH)) or pLenti CMV rtTA3 Hygro (Addgene catalogue number 26730) for transfection of HEK293T cells in Optimem medium (Thermo Fisher Scientific) using lipofectamine 2000. The transfection mix was incubated overnight and the medium replaced the next day. Supernatants were collected on the next two consecutive days upon centrifugation, and cleared through a 0.22-μm filter unit (Stericup, Millipore), before the viruses were aliquoted and frozen at −80 °C. HeLa cells were transduced with 1 ml of viral particles of pLenti CMV rtTA3 Hygro. Following infection, the cells were selected with hygromycin (200 μg ml^{-1}) for 5 days, before they were infected again with the PP7–GFP viruses. GFP-positive clones with similar GFP intensity were isolated with a FACSAria Fusion sorter by EPFL's flow cytometry core facility.

Cloning of TERRA constructs

TERRA constructs were cloned in the pTRE2puro vector of Clontech's TET-ON system without the corresponding polyA region. The PP7 stem-loops were amplified from Addgene plasmid #61762 (a gift from D. Larson) and introduced into pTRE2puro through in-fusion cloning. To amplify the TTAGGG sequence, we performed PCR using the Phusion Green Hot Start II high-fidelity DNA polymerase (F537S) with no template in a reaction containing: 1× GC Phusion buffer, 0.2 mM dNTPs, 0.4 μM primer 5′-TTAGGGTTAGGGTTAGGGTTAGGGTTAGGG-3′, 0.4 μM primer 5′- CCCTAACCCTAACCCTAACCCTAACCCTAA-3′, and 2 U of polymerase. The PCR consisted of 30 s at 98 °C followed by 10 cycles at 98 °C for 5 s, 60 °C for 10 s, and 72 °C for 15 s. DNA products of variable size were fractionated on a 1.2% agarose gel, and the desired size was excised, extracted with a QIAquick gel extraction kit, and cloned into the pTRE2puro vector containing the 24 copies of PP7 stem-loops. Subtelomeric sequences were amplified using a high-fidelity polymerase from phenol–chloroform-extracted genomic DNA from HeLa cells, and introduced into the corresponding vectors through in-fusion cloning. All constructs were verified by restriction digestion and sequencing. The plasmids were amplified in a homologous-recombination-deficient *E. coli* strain (Stbl3) at 30 °C. All of the primers are listed in Extended Data Table 1.

Generation of integrated TERRA cell lines

The integration of TERRA constructs into the AAVS1 locus was performed as described[22]. The guide RNA for AAVS1 (5′-ACCCCACAG TGGGGCCACTA-3′) and its complementary strand were annealed, and cloned into the pSpCas9(BB)-2A-Puro plasmid acquired from Addgene (catalogue number 48139). The donor template encompassed roughly 800 base pairs of homology arms for AAVS1, which were amplified from HeLa genomic DNA, and cloned into the plasmids containing the control PP7 stem-loop construct and the different TERRA transgenes. HeLa cells were transfected with both the gRNA/Cas9 and donor template vectors. Individual clones were screened by PCR for the presence of the transgene in the AAVS1 locus.

Immunofluorescence and FISH

Cells were grown on glass coverslips by following the culture conditions above. The coverslips were washed twice with 1× phosphate-buffered saline (PBS), fixed with 4% paraformaldehyde for 10 min at room temperature, and washed twice with 1× PBS. The cells were then permeabilized in 1× detergent solution for 5 min (0.1% Triton X-100, 0.02% SDS in 1× PBS), followed by pre-blocking with 2% bovine serum albumin (BSA) in 1× PBS for 10 min. Next the cells were blocked with 10% normal goat serum in 2%BSA/1× PBS for 30 min at room temperature. Coverslips were incubated with primary and then secondary antibodies in blocking solution for 90 min each time at room temperature, and fixed with 4% paraformaldehyde for 5 min at room temperature; the samples were then dehydrated with increasing concentrations of ethanol. For FISH staining, the cells were incubated with hybridization solution containing 10 mM Tris–HCl pH 7.4, 70% formamide, 0.5% blocking reagent and 1/1,000 Cy3 probe, denatured at 80 °C for 3 min, and hybridized for 3 h at room temperature. The cells were washed with wash 1 (10 mM Tris–HCl pH 7.4, 70% formamide) and wash 2 (0.1 M Tris–HCl pH 7.4, 0.15 M NaCl, 0.08% Tween-20) twice, stained with 4′,6-diamidino-2-phenylindole (DAPI), and dehydrated with ethanol. Images were acquired on an Upright Zeiss Axioplan or on a Zeiss LSM700 equipped with an AxioCam MRm B/W. Images were processed and analysed with ImageJ and Adobe Photoshop. All statistical analysis was performed using GraphPad Prism. All figures were created in Adobe Illustrator.

Telomeric FISH on metaphase spreads

Cells were treated with 0.05 μg ml^{-1} demecolcine for 2 h, collected and incubated in hypotonic solution (0.075 M KCl) at 37 °C for 8 min. Swollen cells were collected and fixed in ice-cold methanol:acetic acid (3:1) overnight at 4 °C. The next day, 100 μl of cell suspension was dropped onto slides, incubated at 70 °C for 1 min and air-dried overnight at room temperature. FISH staining was performed as above.

Telomere length analysis

HeLa genomic DNA was isolated with the Wizard genomic DNA purification kit according to the manufacturer's instructions (Promega). Then, 6 μg of genomic DNA was digested with 30 U of *Hinf*I and *Rsa*I overnight at 37 °C. The digested DNA was mixed with 6× MassRuler DNA-loading dye (Thermo Fisher Scientific), loaded on a 0.8% agarose gel in 1× Tris–borate–EDTA (TBE) buffer, and fractionated by gel electrophoresis at 2 V cm^{-1} for 20 h. The gels were dried for two hours at 50 °C in vacuum, treated with denaturation buffer (0.5 M NaOH, 1.5 M NaCl) and neutralization buffer (0.5 M Tris-HCl pH 7.5, 1.5 M NaCl), and then pre-hybridized with Church buffer for 1 h at 50 °C. The gels were hybridized overnight at 50 °C with a randomly labelled TeloC probe as described[23]. The gels were washed for 1 h at 50 °C with 4× saline sodium

citrate (SSC), 4× SSC 0.1% SDS, and 2× SSC 0.1%SDS, exposed to a phosphorimager screen and analysed on a Typhoon phosphorimager (GE).

RT–qPCR

For RT–qPCR of TERRA, 3×10^6 cells were harvested following transfection of the chimaeric TERRA constructs. RNA was isolated with a NucleoSpin RNA kit (Macherey-Nagel). RT–qPCR for 15qTERRA was carried out using our previously described protocol[24]. To assess messenger RNA levels following siRNA transfections, we used ThermoFisher Scientific's SuperScript III reverse transcriptase and Power SYBR Green PCR master mix on an Applied Biosystems 7900HT fast real-time system according to the manufacturer's instructions.

Western blotting

Antibodies are listed in Extended Data Table 2. Protein samples were mixed with 2× Laemmli buffer, boiled for 5 min at 95 °C, run on 4–15% SDS–PAGE precast gels (Mini-PROTEAN TGX Gels, BioRad), transferred to nitrocellulose blotting membranes (Amersham), blocked with blocking solution (3% BSA in 1× PBS, 0.1% Tween-20), and incubated overnight at 4 °C with the corresponding primary antibody. Membranes were washed three times for 5 min each with 1× PBS plus Tween (PBST) buffer, and then incubated for 1 h at room temperature with horseradish-peroxidase-conjugated secondary antibodies (Promega) in blocking solution. Membranes were washed again three times for 5 min with 1× PBST before revealing them with a chemiluminescence detection kit (Western bright electrochemiluminescence, Advansta) and analysing them on a Vilber Fusion FX imaging system.

DNA–RNA immunoprecipitation

Cells at roughly 40% confluence in 6-well plates were transfected first with siRNAs and then, the next day, with plasmids. The cells were harvested on ice 48 h later, counted on a CASY cell counter and washed with 1× PBS; samples were taken for DRIP and western blot analysis. For DRIP, 10^7 cells were dissolved in 175 µl of ice-cold RLN buffer (50 mM Tris-HCl pH 8.0, 140 mM NaCl, 1.5 mM $MgCl_2$, 0.5% NP-40, 1 mM dithiothreitol (DTT), and 100 U ml^{-1} RNasIN PLUS), incubated on ice for 5 min, and centrifuged (300*g*, 2 min, 4 °C). The nuclei were lysed in 500 µl RA1 buffer (NucleoSpin RNA, Macherey-Nagel) containing 5 µl of β-mercaptoethanol, and homogenized by passing them through a 20G × $1^{1/2}$ syringe (0.9 mm × 40 mm). The nucleic-acid-containing extracts were mixed with 250 µl H_2O and 750 µl phenol:chloroform:isoamylalcohol (25:24:1) in a Phase Lock Gel heavy (5PRIME) and centrifuged (13,000*g*, 5 min, room temperature). The upper aqueous phase was mixed with 750 µl of ice-cold isopropanol, with addition of NaCl to 50 mM, then incubated on ice for 30 min; precipitated nucleic acids were collected by centrifugation at 10,000*g* for 30 min at 4 °C. The pellets were washed twice with 70% ice-cold ethanol, air-dried, dissolved in 130 µl of H_2O, and sonicated on a Covaris system (10% duty factor, 200 cycles per burst, for 180 s, with an AFA intensifier) to obtain fragments of 100–500 bp. Next, 90 µg of sonicated nucleic acids were mixed with RNaseH1 or H_2O in RNaseH1 buffer (20 mM HEPES-KOH pH 7.5, 50 mM NaCl, 10 mM $MgCl_2$, 1 mM DTT) and incubated at 37 °C for 90 min. The samples were diluted ten times in DIP-1 buffer (10 mM HEPES-KOH pH 7.5, 275 mM NaCl, 0.1% Na-deoxycholate, 0.1% SDS, 1% Triton X-100) and pre-cleared with 80 µl of sepharose protein G beads for 1 h, on a rotating wheel, at 4 °C. One per cent of the nucleic acids were kept as input. Half of the samples (roughly 45 µg of nucleic acids) were incubated with 3 µg of S9.6 antibody or mouse IgG and 40 µl of sepharose protein G beads on a rotating wheel at 4 °C overnight. The next day the samples were washed for 5 min on a rotating wheel at 4 °C with DIP-2 (50 mM HEPES-KOH pH 7.5, 140 mM NaCl, 1 mM EDTA pH 8.0, 1% Triton X-100, 0.1% Na-deoxycholate), DIP-3 (50 mM HEPES-KOH pH 7.5, 500 mM NaCl, 1 mM EDTA pH 8.0, 1% Triton-X100, 0.1% Na-deoxycholate), DIP-4 (10 mM Tris-HCl pH 8.0, 1 mM EDTA pH 8.0, 250 mM LiCl, 1% NP-40, 1% Na-deoxycholate), and TE buffer (10 mM Tris-HCl pH 8.0, 1 mM EDTA pH 8.0). The samples were digested at 65 °C overnight with 10 µg ml^{-1} RNase (DNase-free (Roche)) in a buffer containing 20 mM Tris-HCl pH 8.0, 1% SDS, 0.1 M $NaHCO_3$, 0.5 mM EDTA pH 8.0. The DNA was isolated using the Qiagen PCR clean-up kit. The DNA was pipetted onto a positively charged nylon membrane (Amersham Hybond N+) and telomeric DNA was detected with a telomeric probe as described[25].

RNA immunoprecipitation

Cells were grown to roughly 70% confluence in 15-cm dishes, harvested on ice, counted on a CASY cell counter, washed with 1× PBS, and lysed in RNA-immunoprecipitation RLN buffer (50 mM Tris-HCl pH 8.0, 140 mM NaCl, 1.5 mM $MgCl_2$, 0.5% NP-40, 1 mM DTT, 400 U ml^{-1} RNasIN PLUS, and protease inhibitors (Complete, Roche)). The lysates were pre-cleared with Dynabeads plus protein G for 1 h on a rotating wheel at 4 °C, and incubated overnight with 6 µg of the corresponding antibody on a rotating wheel at 4 °C. Next 35 µl of Dynabeads protein G (ThermoFisher Scientific) that had been preblocked with transfer RNA were added to each mixture and incubated for 2 h on a rotating wheel at 4 °C; this was followed by five washes with RLN buffer supplemented with 6 mM EDTA pH 8.0. The RNA was eluted in 1% SDS, 5 mM EDTA pH 8.0, and 5 mM β-mercaptoethanol at 42 °C for 30 min, followed by 30 min at 65 °C. The RNA was purified using the RNA clean-up protocol of the NucleoSpin RNA kit (Macherey-Nagel). The RNA was denatured at 65 °C for 3 min and pipetted on a positively charged nylon membrane (Amersham Hybond N+). TERRA and U1 snRNA were detected with corresponding probes as described[26].

EMSA

RAD51 protein was purified[27] and diluted in dilution buffer (25 mM Tris-HCl (pH 7.5), 10% (*v*/*v*) glycerol, 0.5 mM EDTA, 50 mM KCl, 1 mM DTT and 0.01% NP40). Increasing concentrations of RAD51 were incubated with 20 nM Cy3-labelled 41mer TERRA (5′-UUAGGGUUAGGGUUAGGGUUAGGGUUAGGGUUAGG-3′), 41mer TelDNA(5′-TTAGGGTTAGGGTTAGGGTTAGGGTTAGGGTTAGG-3′), 41mer non-TelRNA (5′-AGUAUAUAUGAGUAAACUUGGUCUGACAGUUACCAAUGCUU-3′) or 40mer non-TelDNA (5′-AAATTAACAAGTATAATAAGAA ATAGAAACAAGAAATAGA-3′) substrate at 37 °C for 10 min in 10 µl of buffer D (50 mM Tris-HCl (pH 7.5), 50 mM KCl, 1 mM $MgCl_2$, 1 mM ATP). Reaction mixtures were then crosslinked with 0.01% glutaraldehyde for 10 min. Products were resolved using 0.8% TBE agarose gels supplemented with 10 mM KCl at 4 °C for 50 min (6.5 V cm^{-1}). Gels were imaged on a FLA-9000 scanner (Fujifilm) and quantified with Multi Gauge version 3.2 (Fujifilm).

Stability EMSA

Fluorescently labelled 41mer TERRA or 41mer TelDNA substrates (20 nM) were incubated with indicated concentrations of RAD51 at 37 °C for 10 min in 50 mM Tris-HCl (pH 7.5), 50 mM KCl, 1 mM $MgCl_2$ and 1 mM ATP. To challenge assembled RAD51–ssDNA complexes, increasing concentrations of unlabelled 49mer competitor ssDNA (5′-CCTGTTCAAACGCACATATTAAGCATTTC CTGTCATTG GCGGCTAATTC-3′) were added and incubated for another 10 min at 37 °C. Products were crosslinked with 0.005% glutaraldehyde for a further 10 min and resolved using a 0.8% TBE agarose gel supplemented with 10 mM KCl at 4 °C for 50 min (6.5 V cm^{-1}). Gels were imaged on a FLA-9000 scanner (Fujifilm) and quantified with Multi Gauge version 3.2 (Fujifilm).

Assays for R-loop/D-loop formation

Fluorescently labelled 41mer TERRA or 41mer TelDNA (50 nM) were pre-incubated for 10 min at 37 °C with increasing concentrations of RAD51 in 50 mM Tris-HCl (pH 7.5), 1 mM $MgCl_2$ supplemented with 1 mM $CaCl_2$ and 1 mM adenylyl-imidodiphosphate (AMP–PNP). The reaction was started by adding 600 ng pCR4-TOPO vector containing the 15q

subtelomeric sequence followed by 15 copies of TTAGGG repeats. The mixture was incubated for another 10 min at 37 °C and then stopped by adding SDS (0.1%) and proteinase K (0.1 mg ml^{-1}); this was followed by 3-min incubations at 37 °C. Reaction mixtures were separated on 0.8% agarose gel and analysed as described above for EMSA. For digestion of R-loops by RNaseH, the mixtures were incubated for 1 min with phenylmethylsulfonyl fluoride (PMSF; 2 mM) and with EGTA (1.6 mM) at 37 °C to inhibit proteinase K and chelate calcium ions, respectively. The products were digested with RNaseH1 (6.8 mU μl^{-1}, Thermo Scientific) or RNaseH2 (6.8 mU μl^{-1}, New England Biolabs) for 1 min at 37 °C and resolved as above. For antibody-specific supershift of R-loops, the products were formed as described above for RNaseH digestion (but without EGTA) and then incubated with S9.6 antibodies (0.02 $\mu g\ \mu l^{-1}$) for 2 min at 37 °C and/or anti-mouse horseradish-peroxidase-conjugated antibody.

RNaseH1 digestion of telomeric DNA–RNA hybrids

Fluorescently labelled TERRA or non-telomeric RNAs were mixed with their corresponding complementary ssDNA in annealing buffer (10 mM Tris pH 8.5, 50 mM NaCl, 1 mM EDTA). To form DNA–RNA hybrids, the mixture was heated for 5 min at 95 °C, and then gradually cooled to room temperature. The DNA–RNA hybrid (40 nM) was cleaved by RNaseH1 (6.8 mU μl^{-1}) in the presence or absence of 1 mM $CaCl_2$ for 10 min at 37 °C in 50 mM Tris (pH 7.5), 1 mM $MgCl_2$ and 1 mM AMP–PNP. The reaction was stopped by adding SDS/proteinase K, and then incubated for 10 min at 37 °C. Reaction mixtures were loaded on 10% PAGE gel, separated by electrophoresis (90 V for 60 min at 4 °C), scanned using an Image Reader FLA-9000 scanner and quantified by MultiGauge version 3.2 software.

Supershift of DNA–RNA hybrid with S9.6 antibody

Fluorescently labelled TERRA and non-telomeric DNA–RNA hybrids (40 nM) were incubated with 0.015 $\mu g\ \mu l^{-1}$ of S9.6 antibody for 10 min at 37 °C, then crosslinked with 0.01% glutaraldehyde for 10 min at 37 °C and resolved using 0.8% TBE agarose gel at 4 °C for 50 min (6.5 V cm^{-1}). Gels were imaged on a FLA-9000 scanner (Fujifilm) and quantified with Multi Gauge version 3.2 (Fujifilm).

Reporting summary

Further information on research design is available in the Nature Research Reporting Summary linked to this paper.

Data availability

The data that support the findings of this study are available from the corresponding authors upon reasonable request. Source data are provided with this paper.

22. Ran, F. A. et al. Genome engineering using the CRISPR-Cas9 system. *Nat. Protocols* **8**, 2281–2308 (2013).
23. Grolimund, L. et al. A quantitative telomeric chromatin isolation protocol identifies different telomeric states. *Nat. Commun*. **4**, 2848 (2013).
24. Feretzaki, M. & Lingner, J. A practical qPCR approach to detect TERRA, the elusive telomeric repeat-containing RNA. *Methods* **114**, 39–45 (2017).
25. Porro, A. et al. Functional characterization of the TERRA transcriptome at damaged telomeres. *Nat. Commun*. **5**, 5379 (2014).
26. Porro, A., Feuerhahn, S. & Lingner, J. TERRA-reinforced association of LSD1 with MRE11 promotes processing of uncapped telomeres. *Cell Rep*. **6**, 765–776 (2014).
27. Špírek, M. et al. Human RAD51 rapidly forms intrinsically dynamic nucleoprotein filaments modulated by nucleotide binding state. *Nucleic Acids Res*. **46**, 3967–3980 (2018).

Acknowledgements We thank D. Larson (NIH), D. Bishop (Univ. Chicago), V. Simanis (EPFL), P. Gönczy (EPFL) and D. Trono (EPFL) for providing material. We also thank the members of the BIOP core facility at EPFL, members of the Gönczy laboratory and M. Spirek for technical support and advice and J. Cibulka for recombinant mutant RAD51 protein. M.F. was supported by the European Union's Horizon 2020 research and innovation programme under Marie Skłodowska-Curie grant agreement 702824. J.L.'s laboratory was supported by the Swiss National Science Foundation (SNFS grant 310030_184718), the SNFS-funded National Centres of Competence in Research (NCCR) RNA and disease network (grant 182880), and EPFL. L.K.'s laboratory was supported by the European Structural and Investment Funds, Operational Programme Research, Development and Education 'Preclinical Progression of New Organic Compounds with Targeted Biological Activity' (Preclinprogress) (CZ.02.1.01/0.0/0.0/16_025/0007381); a Wellcome Trust Collaborative Grant 206292/E/17/Z; the Czech Science Foundation (GACR 17-17720S); and the National Program of Sustainability II (MEYS CR, project number LQ1605). Both J.L. and L.K. were also supported by the European Union's Horizon 2020 research and innovation programme under grant agreement 812829.

Author contributions M.F. and J.L. conceived the study. M.F. and R.V.F. executed all cell and molecular biology experiments. M.P. performed all biochemistry experiments and T.L. some EMSA experiments. L.K. conceived the RAD51-based biochemistry experiments and advised on the text. J.L. and M.F. wrote the paper.

Competing interests The authors declare no competing interests.

Additional information

Supplementary information is available for this paper at https://doi.org/10.1038/s41586-020-2815-6.

Correspondence and requests for materials should be addressed to L.K. or J.L.

Peer review information *Nature* thanks the anonymous reviewers for their contribution to the peer review of this work.

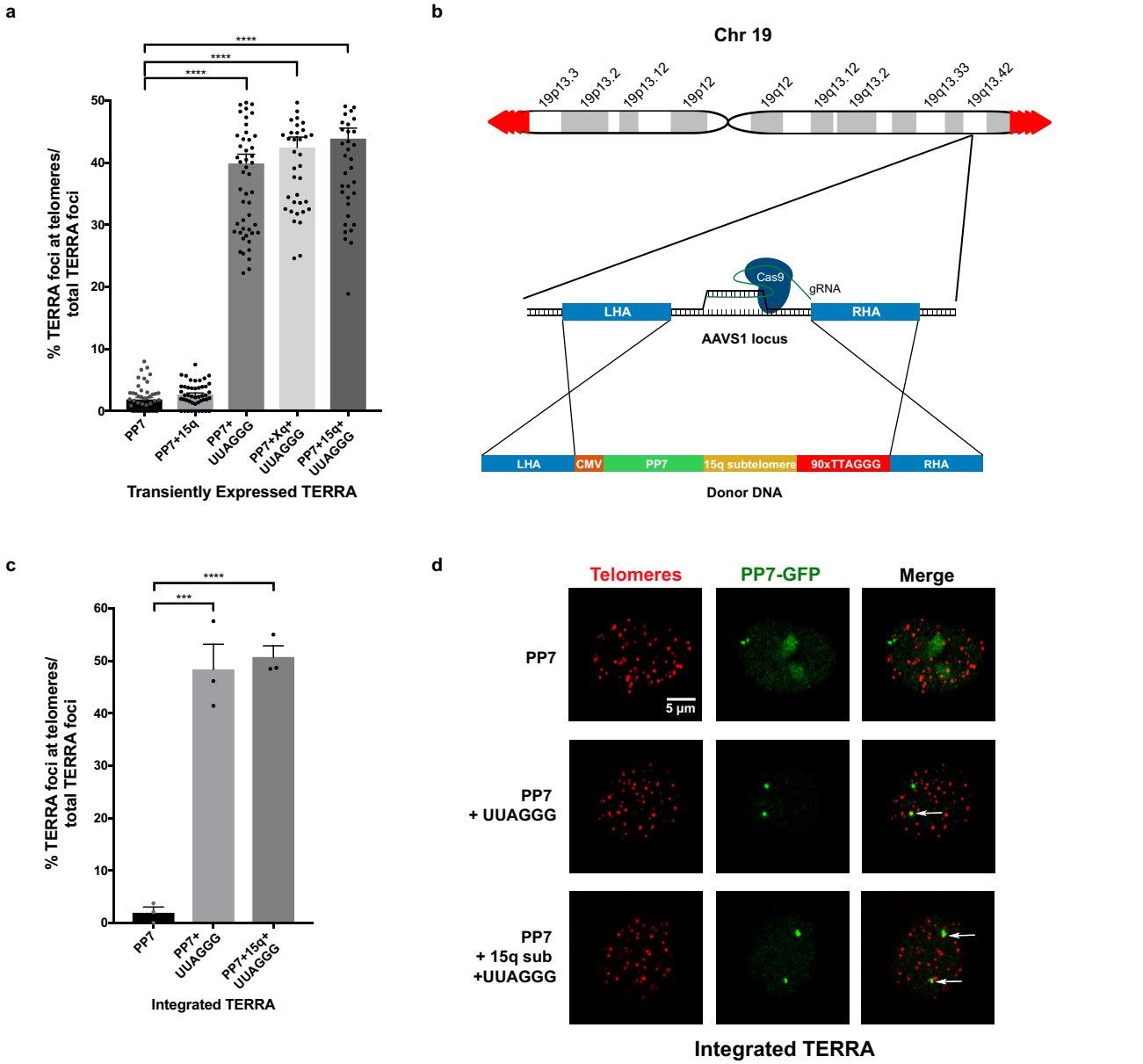

Extended Data Fig. 1 | Co-localization of transgenic TERRA with telomeres. **a**, Quantification of co-localization of transgenic RNA foci expressed from plasmids with telomeres. **b**, Strategy for targeting the AAVS1 locus through CRISPR–CAS9 to integrate chimaeric TERRA constructs into the genome. LHA and RHA, left and right homology arms. **c**, Quantification of co-localization of transgenic RNA foci with telomeres when TERRA was expressed from the AAVS1 locus. **d**, Confocal images obtained when TERRA was expressed from the AAVS1 locus. For **a**, **c**, $n = 3$ biologically independent experiments; data are mean ± s.d.; two-tailed unpaired *t*-test: $^{***}P < 0.001$; $^{****}P < 0.0001$.

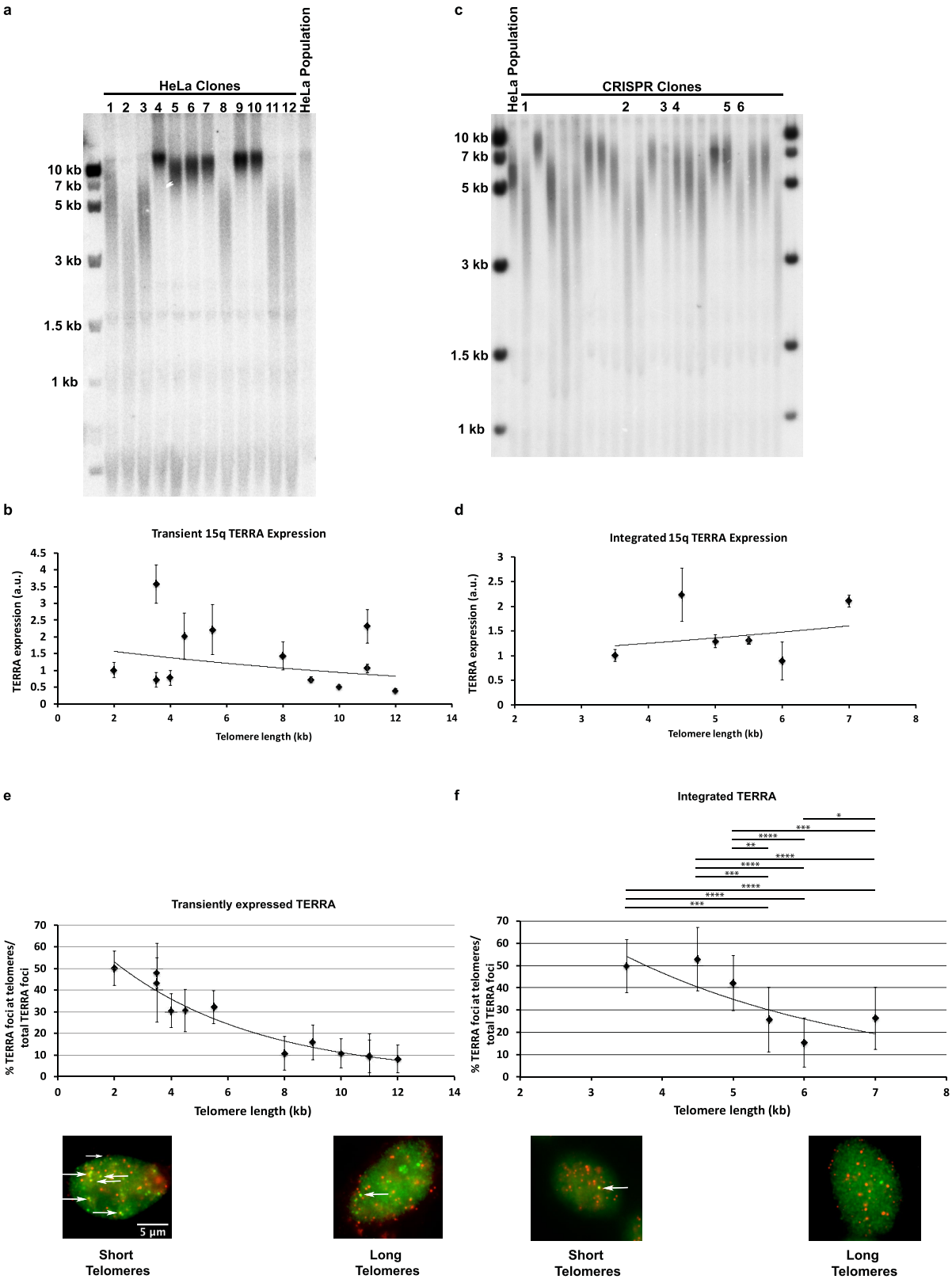

Extended Data Fig. 2 | TERRA associates preferentially with short telomeres. a, TRF analysis of HeLa clones used for transient expression of TERRA. **b**, **d**, TERRA expression levels measured by RT–qPCR relative to the levels of TERRA in the clone with the shortest telomeres. $n = 3$ biologically independent experiments; data are means ± s.d. **c**, TRF analysis of HeLa clones expressing transgenic TERRA from the AAVS1 locus. **e**, HeLa clones of different telomere lengths were transiently transfected with the PP7–15qTERRA construct and co-localization was assessed by immunofluorescence with FISH (bottom). White arrows indicate co-localization of PP7 foci with the telomeric signal. The percentage of TERRA foci that co-localized with telomeres is plotted as a function of telomere length (top). Random colocalization events (roughly 3%) were not subtracted. **f**, Co-localization events as in **e** but for PP7–15qTERRA expressed from the AAVS locus on chromosome 19. $n = 3$ biologically independent experiments; data are means ± s.d. Significant differences are indicated. Two-tailed unpaired *t*-tests were used to calculate *P*-values: $^{*}P < 0.05$; $^{**}P < 0.01$; $^{***}P < 0.001$; $^{****}P < 0.0001$.

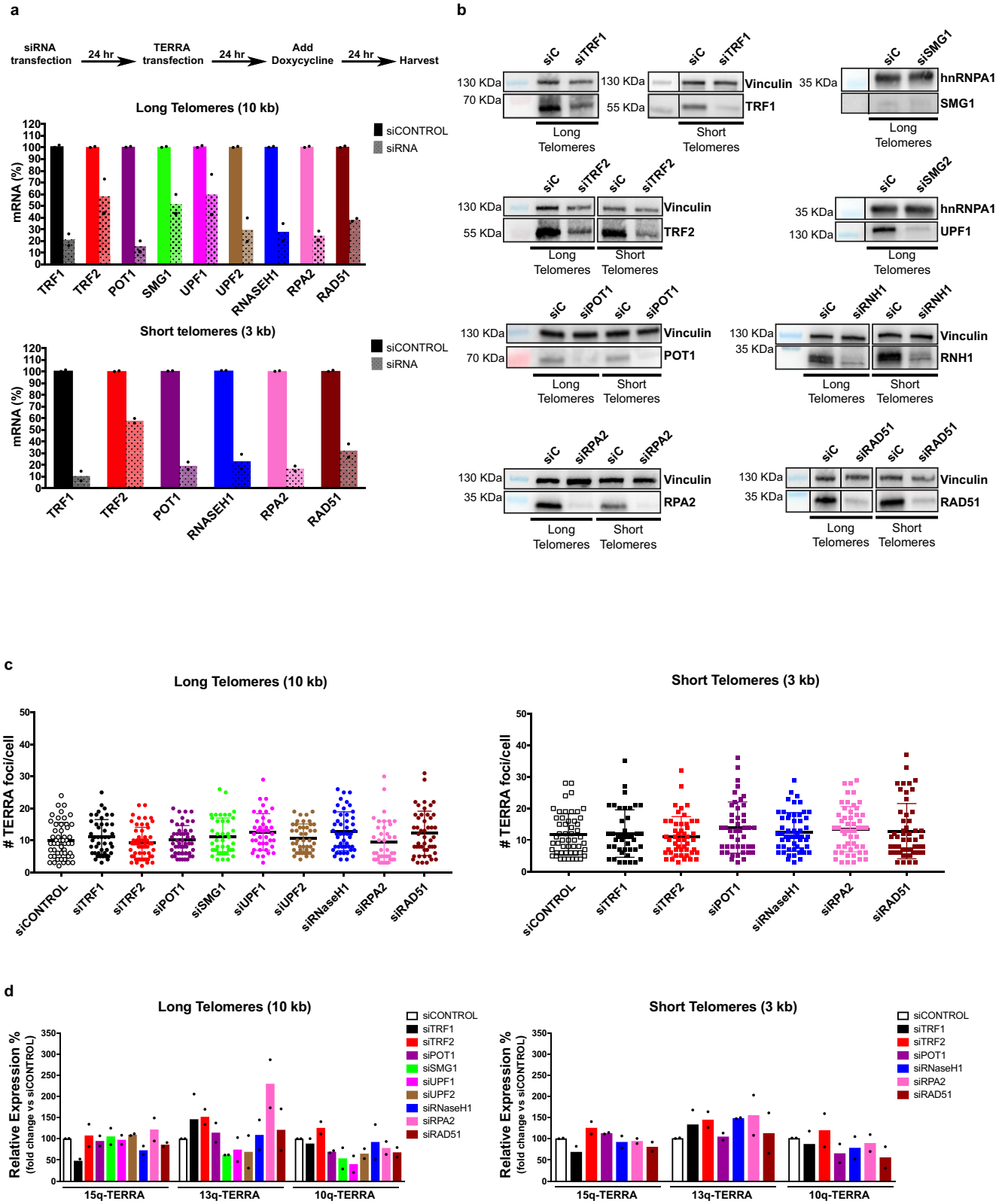

Extended Data Fig. 3 | Depletion of factors regulating TERRA trafficking. **a**, Timeline of transfections and cell harvesting. mRNA levels were determined by RT–qPCR for long-telomere and short-telomere cell lines. **b**, For the second replicate of each siRNA screen, the level of depletion was also evaluated on western blots. Vinculin and hnRNPA1 were used as loading controls. **c**, Numbers of TERRA foci per cell are plotted for each depleted factor. $n = 2$ biologically independent experiments; at least 40 nuclei were analysed per condition. **d**, Quantification of endogenous TERRA stemming from the ends of chromosomes 15q, 13q and 10q upon depletion of the indicated factors relative to the negative control (siCONTROL). $n = 2$ biologically independent experiments.

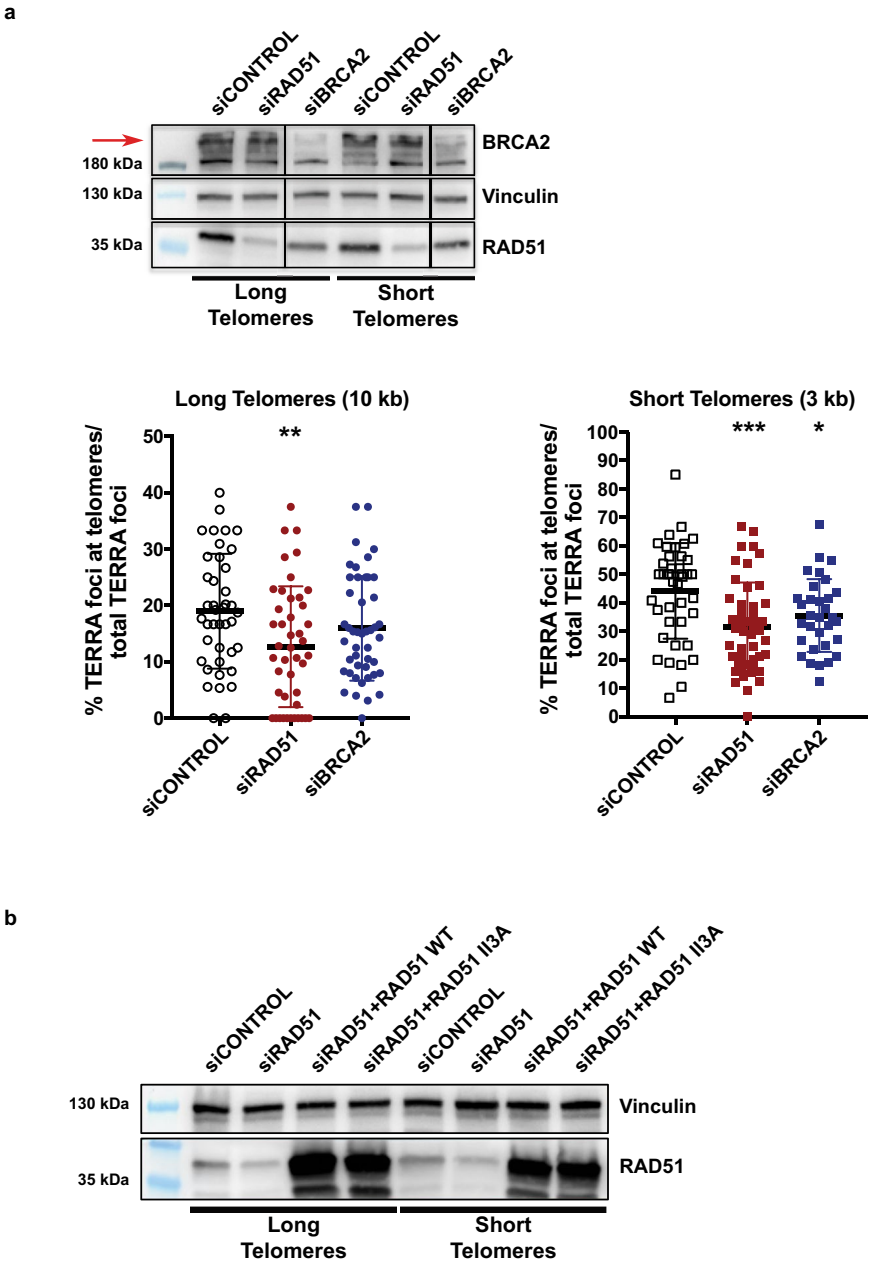

Extended Data Fig. 4 | Depletion of RAD51 and BRCA2, which regulate the association of TERRA with telomeres. a, HeLa clones with long and short telomeres were transfected with siRAD51 and siBRCA2, and then with chimaeric TERRA constructs. Representative immunoblots show RAD51 and BRCA2 depletion, with vinculin as a loading control. Upon depletion, co-localization of TERRA with telomeres was assessed with immunofluorescence–FISH. $n = 2$ biologically independent experiments; at least 54 nuclei were analysed per condition; data are means ± s.d. One-way ANOVA with Dunnett's multiple comparisons test was used, comparing all conditions to siCONTROL: $^{*}P < 0.05$; $^{**}P < 0.01$; $^{***}P < 0.001$. **b**, Detection of endogenous and transgenic RAD51 on a western blot. Endogenous RAD51 was depleted with siRNA, and wild-type (WT) RAD51 or the RAD51 II3A mutant was expressed from plasmids containing complementary DNA.

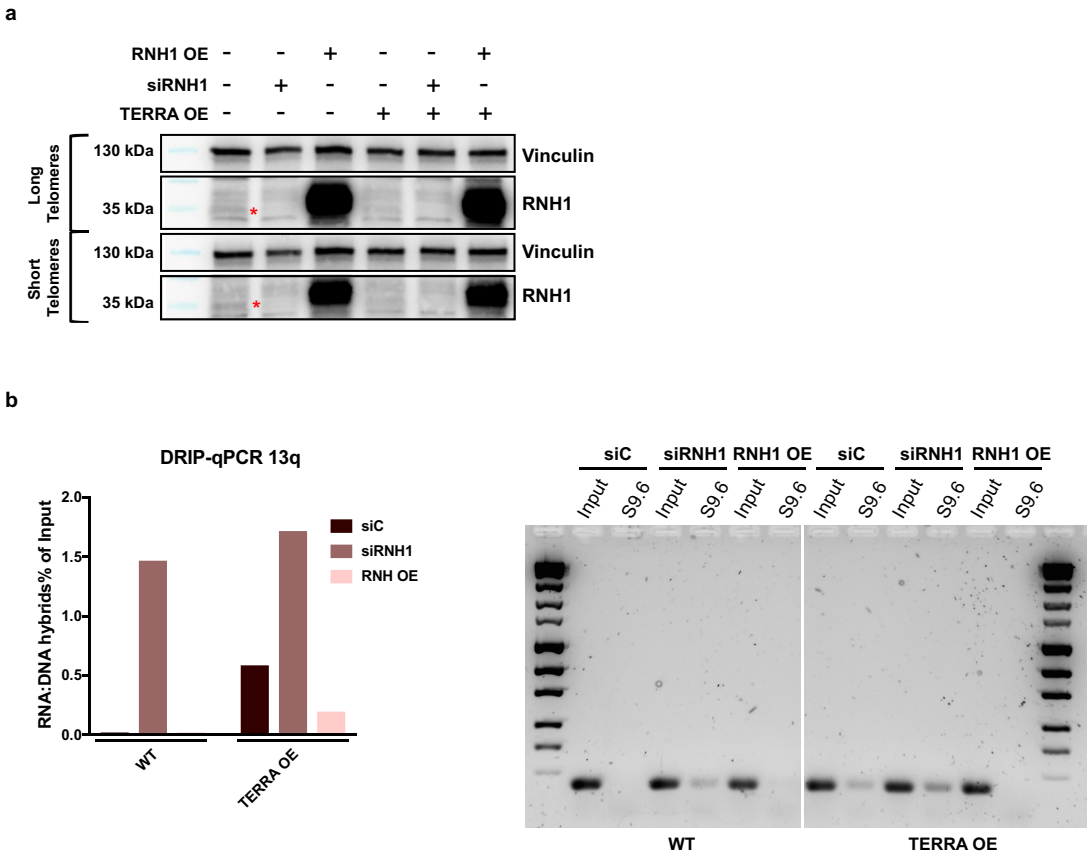

Extended Data Fig. 5 | RNaseH1-regulated formation of telomeric R-loops in *trans*. **a**, RNH1 depletion and overexpression (OE) was assessed by western blotting in cell lines with long and short telomeres and upon TERRA overexpression. **b**, Representative example of one DRIP assay followed by qPCR for the end of chromosome 13q. Left, quantification of RNA–DNA hybrids is expressed as a fraction of input. Right, the amplified DNA was run on a gel, then isolated and sequenced.

a

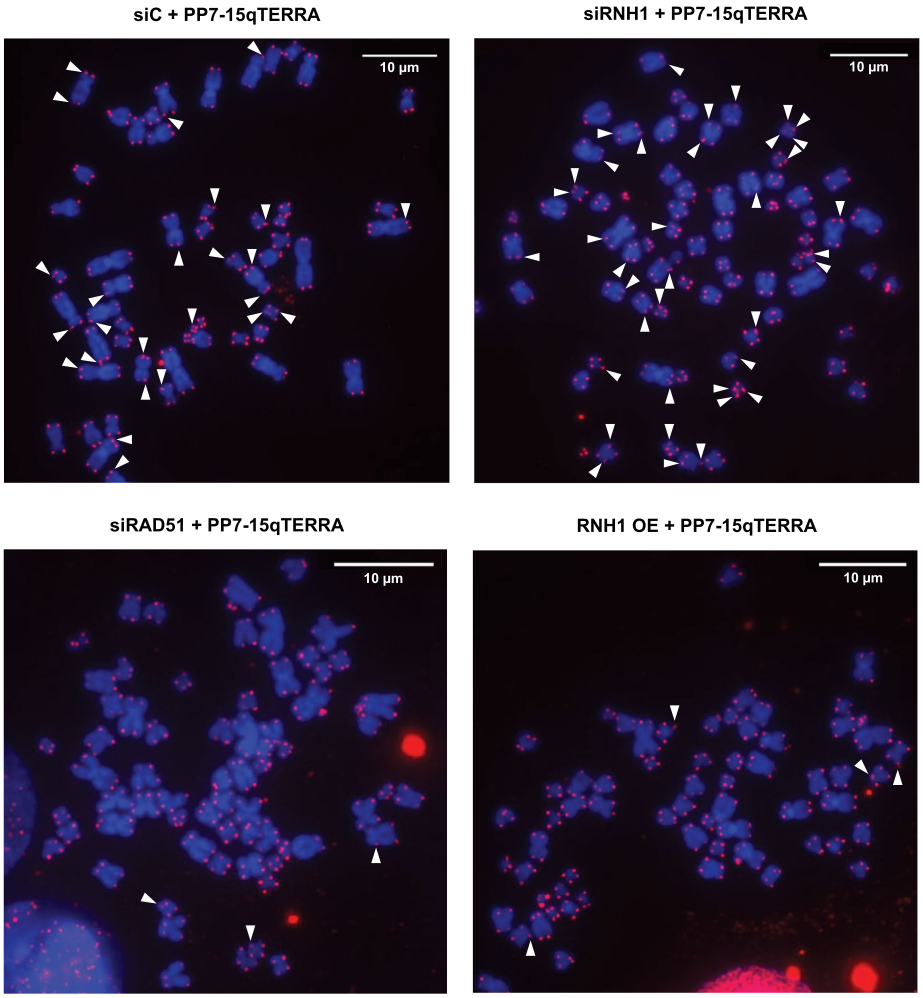

b

Plasmid	Metaphases scored	Telomere Fragility (mean % ± SEM)
PP7	n=59	2.7 ± 0.2
PP7+UUAGGG	n=58	5.4 ± 0.4
PP7+15q+UUAGGG	n=60	4.6 ± 0.2
PP7+Xq+UUAGGG	n=58	5.1 ± 0.3

c

	Condition	Metaphases scored	Telomere Fragility (mean % ± SEM)
+ PP7-15qTERRA	siC	n=64	5.3 ± 0.4
	siRNH1	n=69	7.1 ± 0.3
	siRAD51	n=64	3.4 ± 0.3
	RNH1 OE	n=64	2.8 ± 0.2

Extended Data Fig. 6 | Transgenic TERRA expressed from plasmids induces telomere fragility. a, Representative examples of metaphase chromosomes stained with FISH to visualize telomeres. DNA is stained with DAPI. Fragile telomeres are indicated by white arrowheads. **b**, Quantification of telomere fragility. **c**, Quantification of telomere fragility in cells expressing PP7–15qTERRA in which expression of RNaseH1 (RNH1) and RAD51 was manipulated as indicated. For **b**, **c**, the numbers of metaphases scored over three biologically independent experiments are indicated for each condition as *n*.

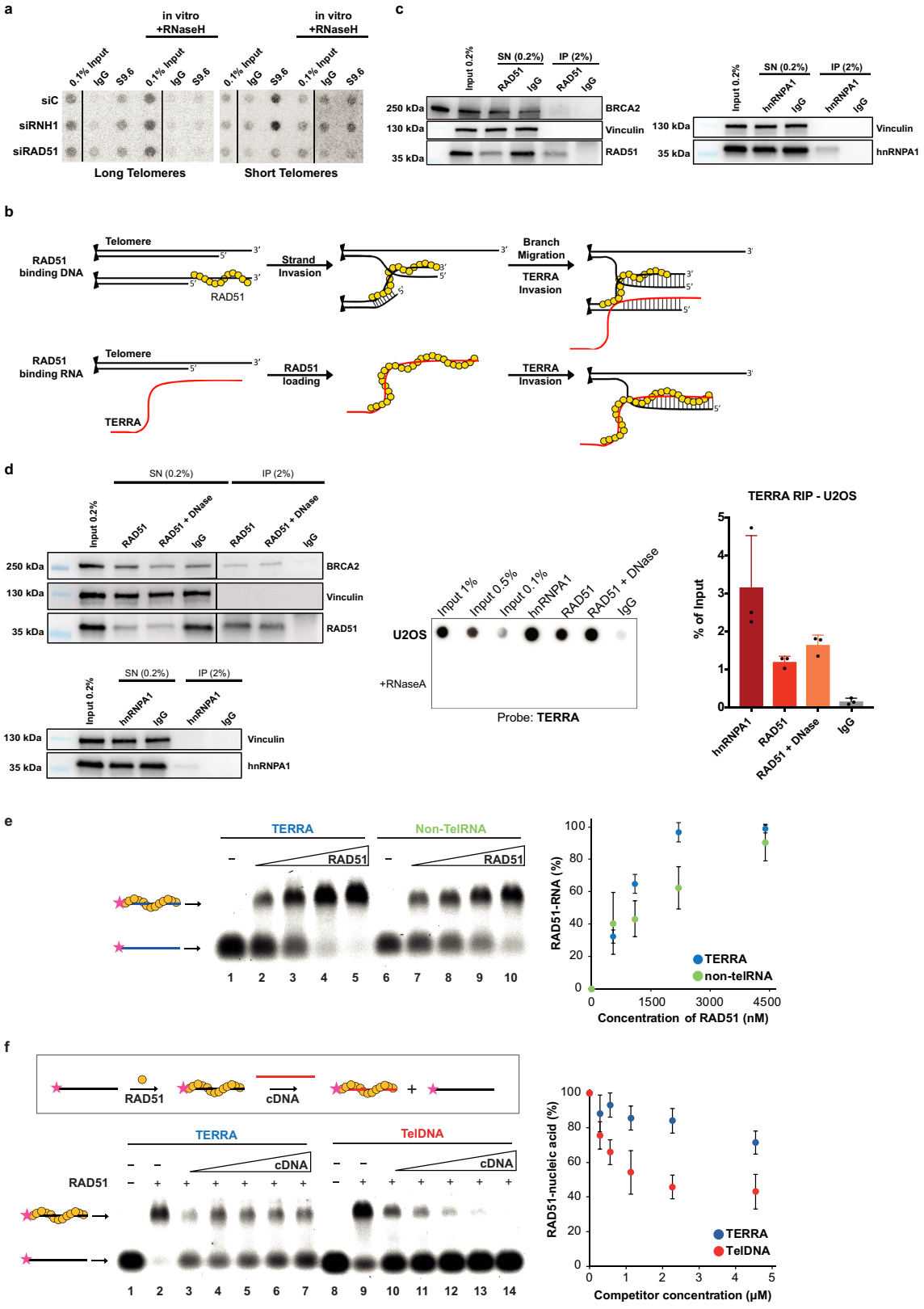

Extended Data Fig. 7 | See next page for caption.

Extended Data Fig. 7 | RAD51 binds TERRA and promotes R-loop formation. **a**, Detection of endogenous telomeric R-loops on dot-blots as in Fig. 2a. Cells were transfected with siCONTROL (siC), siRNH1 or siRAD51. **b**, Possible models for the roles of RAD51 in mediating TERRA–telomere associations. Upper row, RAD51 binds telomeric single-stranded DNA, inducing strand invasion of another telomere. TERRA hybridizes to the displaced strand upon branch migration. Lower row, RAD51 binds TERRA directly and initiates homology search and strand invasion by TERRA at a telomere. **c**, Western blot analysis of RAD51 and hnRNPA1 upon immunoprecipitation (IP) of native RNA (see Fig. 3a for RNA analysis). SN, supernatant. **d**, Native Immunoprecipitation of RNA was performed in U2OS cell extracts, demonstrating the association of TERRA with RAD51 and hnRNPA1. $n = 3$ biologically independent experiments; data are means ± s.d. **e**, Affinity of RAD51 for TERRA and non-telomeric-RNA (Non-TelRNA) oligonucleotides. Quantification is shown on the right. $n = 3$ independent experiments; data are means ± s.d. **f**, Top, stability EMSA assay. Bottom, 20 nM TERRA (lanes 2-7) or TelDNA (lanes 9-14) oligonucleotides were pre-bound with RAD51 (2.2 μM or 8.8 μM) and challenged with increasing concentrations of unlabelled competitor ssDNA (cDNA; 0.28 μM, 0.56 μM, 1.13 μM, 2.27 μM or 4.54 μM). Quantification is shown on the right. $n = 3$ independent experiments; data are means ± s.d.

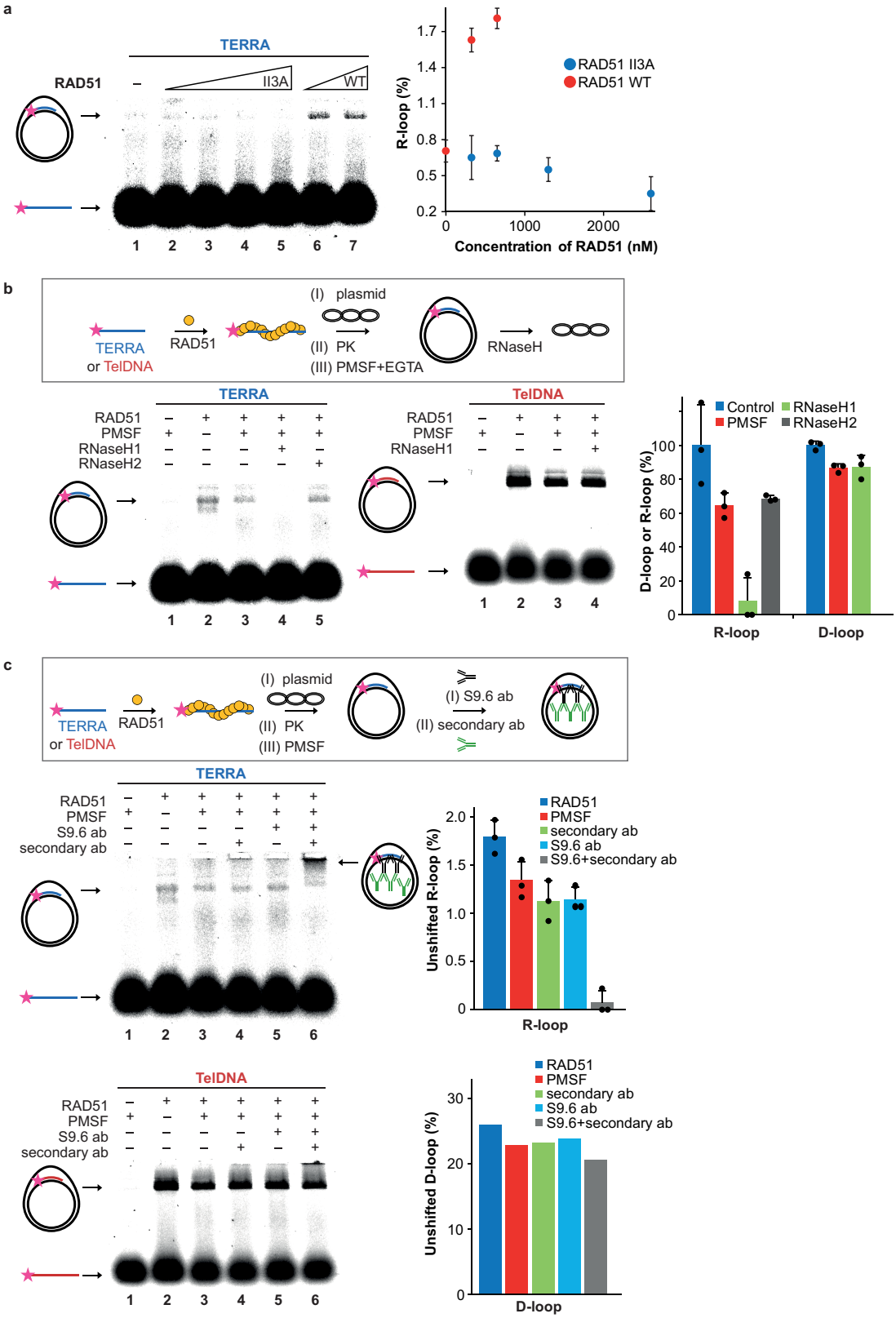

Extended Data Fig. 8 | See next page for caption.

Extended Data Fig. 8 | RAD51 catalyses the formation of canonical R-loops. **a**, Left, the RAD51 II3A mutant (lines 2–5; 325 nM, 650 nM, 1,300 nM or 2,600 nM) or wild-type RAD51 (lines 6 and 7; 325 nM or 650 nM) was incubated with TERRA oligonucleotide substrate (50 nM), and then plasmid containing the homologous region was added. Right, quantification of R-loops in the presence of wild-type RAD51 or RAD51 II3A. $n = 2$ independent experiments; data are means ± s.d. **b**, Top, the R-loop and D-loop assays. After RAD51-mediated R-loop or D-loop formation, proteins were digested with proteinase K (PK), which was then inactivated with PMSF and EGTA. Bottom left, R-loops or D-loops were detected on native gels as indicated. Treatment with RNaseH1, which degrades the RNA moiety in RNA–DNA hybrid structures, eliminates R-loops but has no effect on D-loops. RNaseH2, which cleaves ribonucleotides in DNA, has no effect, as expected. Right, quantification. $n = 3$ independent experiments; data are means ± s.d. **c**, Top, the R-loop and D-loop assays. Middle and bottom, RAD51-mediated R-loops (middle; $n = 3$ independent experiments; data are means ± s.d.), unlike D-loops (n=1 experiment), are recognized by the S9.6 antibody and supershifted in presence of both S9.6 and anti-mouse IgG. Quantification is shown on the right.

Extended Data Table 1 | Oligonucleotides used herein

Primers used for Chimeric TERRA constructs

Name	Forward	Reverse
Amplification of PP7 stem loops	CCGCGGCCCCGAATTCTATCGATACTCGAGATCCTA	GCTGACTAGAGGATCCACACGCGTTCTCGATAATGAA
Amplification of TTAGGG repeats	TTAGGGTTAGGGTTAGGGTTAGGGTTAGGG	CCCTAACCCTAACCCTAACCCTAACCCTAA
Amplification of 15q subtelomere	GAACGCGTGTGGATCATTCTCCTCAGGTCAGACCCG	CTAACCCTAAGGATCCTAACCGTGACCCTGACCCCG
Amplification of Xq subtelomere	GAACGCGTGTGGATCCCGAGTTGCGTTCTCG	CTAACCCTAAGGATCGCACATGAGGAATGTGGGTG
Amplification of AAVS1 left homology arm	TGACCGGTTGCTTTCTCTGACCAGCATTC	GTGTTAACCACTGTGGGGTGGAGGGGAC
Amplification of AAVS1 right homology arm	CGGATATCACTAGGGACAGGATTGGT	GTGATATCCTGTAGGAAGGGGCAGGAGA

Primers used for RT-qPCR

Name	Forward	Reverse
15q TERRA	CAGCGAGATTCTCCCAAGCTAAG	AACCCTAACCACATGAGCAACG
GAPDH	AGCCACATCGCTCAGACAC	GCCCAATACGACCAAATCC
TRF1	CTTGCCAGTTGAGAACGATATACA	CATCAGGGCTGATTCCAAGG
TRF2	GGGTTATGCAGTGTCTGTCGCG	CAGTGGTGTGAGCTCAGCCT
POT1	CCAAGCTCTGGATCAGTATCATT	CATAGTGGTGTCCTCTC AAATAC
SMG1	CCAAGCACCGTTCCAGGAACTG	CTCTCTTGCACCGCTTTCCCAG
UPF1	CGCAGGGCTACATCTCCATGAG	CTCGTCACCAAGGTAACTGTCCTG
UPF2	GGCTGAGTCTGCAGACACAATGC	GCAGCAAGTTGAGAGGACATGGG
RNaseH1	GGCCAGGCCATCCTTTAAATGTAGG	GCTTGTTCAATGGCTTTGCAGGC
RPA2	GCAGGGAACTTTGGTGGGAATAGC	CCCTTCAGGTCTTGGACAAGCC
RAD51	GAGGAAAGGAAGAGGGGAAACCAG	CCCACTCCATCTGCATTAATGGCG
1q subtelomere	CAGCGTCGCAACTCAAATG	CCCTCACCCTCCATGAGTAATA
10q subtelomere	GCATTCCTAATGCACACATGAC	TACCCGAACCTGAACCCTAA
13q subtelomere	GCACTTGAACCCTGCAATACAG	CCTGCGCACCGAGATTCT
15q subtelomere	AACCCTAACCACATGAGCAACG	GCTGCATTAAAGGGTCCAGT

siRNAs

Gene name	Dharmacon catalog number	siRNA sequences
siControl	D-001206-13-20	UAGCGACUAAACACAUCAA, UAAGGCUAUGAAGAGAUAC, AUGUAUUGGCCUGUAUUAG, AUGAACGUGAAUUGCUCAA
siTRF1	M-010542-02	CAAGAUAAACCUAGUGGUA, GGUGAUCCAAAUUCUCAUA, GGAAACUGGUCUAAAAUAC, GCCAGUUGAGAACGAUAUA
siTRF2	M-003546-00	GAAGUGGACUGUAGAAGAA, GGAAGCUGCUGUCAUUAUU, GGAAUCAGCUAUCAAUGUG, GAAGACAGUACAACCAAUA
siPOT1	M-004205-01	AGAAAGAUGUCAACAGCUA, GAGGCAAAGAAUCGAAAUA, CAGGAGUACUAGAAGCCUA, UGCAAGAUCUCCACGUUAA
siSMG1	M-005033-01	GUGAAGAUGUUCCCUAUGA, GAGGUUAGCUGCGGAAAGA, GGUCAGACAUCCACCAGAA, UAACUUGGCUCAGCUGUAU
siUPF1	M-011763-01	GCUCCUACCUGGUGCAGUA, UCAAGGUCCCUGAUAAUUA, GGAAGUCGACCUCCUUUGA, CAAGAUAACAUCACUGUCA
siUPF2	M-012993-01	GGAACGAGAAUUCUUAAUA, GCAUGUACCUUGUGUAGAA, GAAGAUAUUCGAUUAGGAA, GGUCUAGAGAGUUGCGAAU
siRNaseH1	M-012595-00	GCGCAGAGCCGUAUGCAAA, GAGCUAAACAAUCGGAAGA, GCCAGGCCAUCCUUUAAAU, GACAUUCAGUGGAUGCAUG
siRPA2	M-017058-00	GAUCAAUGCACACAUGGUA, CAAAAUAGAUGACAUGACA, GAGUGAAGCAGGGAACUUU, GUGGAACAGUGGAUUCGAA
siRAD51	M-003530-04	GAAGCUAUGUUCGCCAUUA, GCAGUGAUGUCCUGGAUAA, CCAACGAUGUGAAGAAAUU, AAGCUAUGUUCGCCAUUAA
siBRCA2	M-003462-01	GAAACGGACUUGCUAUUUA, GUAAAGAAAUGCAGAAUUC, GGUAUCAGAUGCUUCAUUA, GAAGAAUGCAGGUUUAAUA

Extended Data Table 2 | Antibodies used herein

Antibody	Company	Catalogue No	Dilution (Technique)
Anti-GFP	Home-Made		1:1,000 (IF)
Anti-GFP	Merck Millipore	MAB3580	1:1,000 (IF, WB)
Anti-RAD51	Santa-Cruz	sc-8349	1:1,000 (WB)
Anti-RAD51	ABCAM	ab133534	6 µg (IP)
Anti-BRCA2	Merck Millipore	MAB3580	1:1,000 (WB)
Anti-Vinculin	ABCAM	ab129002	1:10,000 (WB)
Anti-hnRNPA1	Santa-Cruz	sc-32301	1:1,000 (WB), 6 µg (IP)
Anti-RNaseH1	GeneTex	GTX-117624	1:1,000 (WB)
Anti-TRF1	Santa-Cruz	sc-6165R	1:1,000 (WB)
Anti-TRF2	Merck Millipore	05-521	1:1,000 (WB)
Anti-POT1	ABCAM	ab124784	1:1,000 (WB)
Anti-SMG1	Abgent	AP8055a	1:500 (WB)
Anti-UPF1	Bethyl Laboratories	A300-037A	1:1,000 (WB)
Anti-RPA2	ABCAM	ab2175	1:1,000 (WB)
Anti-DNA-RNA Hybrid [S9.6]	Kerafast	ENH001	1 µg / 10 µg nucleic acids (DRIP)
Anti-Rabbit IgG (H+L), HRP Conjugate	Promega	W4011	1:10,000 (WB)
Anti-Mouse IgG (H+L), HRP Conjugate	Promega	W4021	1:10,000 (WB)
Goat anti-Rabbit IgG (H+L) Cross-Adsorbed Secondary Antibody, Alexa Fluor 633	Thermo Fisher	A-21070	1:1,000 (IF)

IF, immunofluorescence; IP, immunoprecipitation; WB, western blot.

nature research

Corresponding author(s): Joachim Lingner

Last updated by author(s): Jun 22, 2020

Reporting Summary

Nature Research wishes to improve the reproducibility of the work that we publish. This form provides structure for consistency and transparency in reporting. For further information on Nature Research policies, see Authors & Referees and the Editorial Policy Checklist.

Statistics

For all statistical analyses, confirm that the following items are present in the figure legend, table legend, main text, or Methods section.

n/a	Confirmed
☐	☒ The exact sample size (*n*) for each experimental group/condition, given as a discrete number and unit of measurement
☐	☒ A statement on whether measurements were taken from distinct samples or whether the same sample was measured repeatedly
☐	☒ The statistical test(s) used AND whether they are one- or two-sided *Only common tests should be described solely by name; describe more complex techniques in the Methods section.*
☒	☐ A description of all covariates tested
☒	☐ A description of any assumptions or corrections, such as tests of normality and adjustment for multiple comparisons
☐	☒ A full description of the statistical parameters including central tendency (e.g. means) or other basic estimates (e.g. regression coefficient) AND variation (e.g. standard deviation) or associated estimates of uncertainty (e.g. confidence intervals)
☐	☒ For null hypothesis testing, the test statistic (e.g. *F*, *t*, *r*) with confidence intervals, effect sizes, degrees of freedom and *P* value noted *Give P values as exact values whenever suitable.*
☒	☐ For Bayesian analysis, information on the choice of priors and Markov chain Monte Carlo settings
☒	☐ For hierarchical and complex designs, identification of the appropriate level for tests and full reporting of outcomes
☒	☐ Estimates of effect sizes (e.g. Cohen's *d*, Pearson's *r*), indicating how they were calculated

Our web collection on statistics for biologists contains articles on many of the points above.

Software and code

Policy information about availability of computer code

Data collection	Microscopy images were acquired on an Upright Zeiss Axioplan or on a Zeiss LSM700 equipped with an AxioCam MRm B/W. The screens were developed on a Typhoon phosphorimager (GE). Western Blot membranes were developed on a Vilber Fusion FX imaging system. EMSA Gels were imaged on a FLA-9000 scanner (Fujifilm) and quantified with Multi Gauge V3.2 (Fujifilm).
Data analysis	Images were processed and analyzed with Image J (2.0.0-rc-69/1.52n). Graphs were prepared in GraphPad Prism 7 (7.0d) and Figures assembled using Adobe Photoshop (21.1.0) and Adobe Illustrator (24.0.3).

For manuscripts utilizing custom algorithms or software that are central to the research but not yet described in published literature, software must be made available to editors/reviewers. We strongly encourage code deposition in a community repository (e.g. GitHub). See the Nature Research guidelines for submitting code & software for further information.

Data

Policy information about availability of data

All manuscripts must include a data availability statement. This statement should provide the following information, where applicable:

- Accession codes, unique identifiers, or web links for publicly available datasets
- A list of figures that have associated raw data
- A description of any restrictions on data availability

All materials and data-sets are available upon request.

Field-specific reporting

Please select the one below that is the best fit for your research. If you are not sure, read the appropriate sections before making your selection.

☒ Life sciences ☐ Behavioural & social sciences ☐ Ecological, evolutionary & environmental sciences

For a reference copy of the document with all sections, see nature.com/documents/nr-reporting-summary-flat.pdf

Life sciences study design

All studies must disclose on these points even when the disclosure is negative.

Sample size	No statistical method was used to pre-determine sample size. Sample sizes were chosen according to commonly used standards in the field. (Azzalin et al. Science. 2007 Nov 2;318(5851):798-801; Vančevska et al. EMBO J. 2020 Apr 1;39(7):e102668) The number of independent experiments are indicated in the legend of each Figure. Proper Negative and whenever possible positive controls were used for each experiment.
Data exclusions	No data was excluded from the analysis
Replication	The screen in Figure 2c was performed in two independent biological replicates. All the other experiments were performed in three independent biological replicates. All the replicates were successful
Randomization	All samples were chosen randomly
Blinding	For Figures 1c, 1d, 2c, 2d, and Ext. Figure 2e, 2f, 4a the researchers were blinded to image acquiring and analysis. For the rest either the differences between samples were obvious making blinding impossible or blinding was not applicable due to the nature of the experiment.

Reporting for specific materials, systems and methods

We require information from authors about some types of materials, experimental systems and methods used in many studies. Here, indicate whether each material, system or method listed is relevant to your study. If you are not sure if a list item applies to your research, read the appropriate section before selecting a response.

Materials & experimental systems

n/a	Involved in the study
☐	☒ Antibodies
☐	☒ Eukaryotic cell lines
☒	☐ Palaeontology
☒	☐ Animals and other organisms
☒	☐ Human research participants
☒	☐ Clinical data

Methods

n/a	Involved in the study
☒	☐ ChIP-seq
☒	☐ Flow cytometry
☒	☐ MRI-based neuroimaging

Antibodies

Antibodies used	See also Table S2: GFP Home-Made GFP Merck Millipore MAB3580 RAD51 Santa-Cruz sc-8349 RAD51 ABCAM ab133534 BRCA2 Merck Millipore MAB3580 Vinculin ABCAM ab129002 hnRNPA1 Santa-Cruz sc-32301 RNaseH1 GeneTex GTX-117624 TRF1 Santa-Cruz sc-6165R TRF2 Merck Millipore 05-521 POT1 ABCAM ab124784 SMG1 Abgent AP8055a UPF1 Bethul Laboratories A300-037A RPA2 ABCAM ab2175 Anti-DNA-RNA Hybrid [S9.6] Kerafast ENH001 Anti-Rabbit IgG (H+L), HRP conjugate, Promega, W4011 Anti-Mouse IgG (H+L), HRP conjugate, Promega, W4021 Goat Anti-Rabbit IgG (H+L) Cross-Absorbed Secondary Antibody, Alexa Fluor 633, ThermoFisher, A-21070
Validation	Validation for each antibody is provided in the manuscript. The specificity of most of them (including the home-made GFP

antibody) was tested upon disappearance of the corresponding band upon siRNA knock down in this study. S9.6 specificity for DNA-RNA hybrids is confirmed by in-vitro treatment with RNAseH1.

Eukaryotic cell lines

Policy information about cell lines

Cell line source(s)	HeLa and HEK293T cell lines were purchased from ATCC. U2OS was purchased from ECACC
Authentication	HeLa and HEK293Tcell lines have not been authenticated by us but the supplier. U2OS cell line was authenticated by measuring the production of c-circles (a known ALT cell line phenotype)
Mycoplasma contamination	All the cell lines were tested negative for mycoplasma
Commonly misidentified lines (See ICLAC register)	No commonly misidentified cell lines were used